DNA-TR-85-156

THEORETICAL STUDY OF THE RADIATIVE AND KINETIC PROPERTIES OF SELECTED METAL OXIDES AND AIR MOLECULES

H. H. Michels
R. H. Hobbs
United Technologies Research Center
400 Main Street
East Hartford, CT 06108

1 May 1985

Technical Report

CONTRACT No. DNA 001-83-C-0044

THIS WORK WAS SPONSORED BY THE DEFENSE NUCLEAR AGENCY
UNDER RDT&E RMSS CODE B322084466 S99QMXBI00025 H2590D.

Prepared for
Director
DEFENSE NUCLEAR AGENCY
Washington, DC 20305-1000

Destroy this report when it is no longer needed. Do not return to sender.

PLEASE NOTIFY THE DEFENSE NUCLEAR AGENCY, ATTN: STTI, WASHINGTON, DC 20305-1000, IF YOUR ADDRESS IS INCORRECT, IF YOU WISH IT DELETED FROM THE DISTRIBUTION LIST, OR IF THE ADDRESSEE IS NO LONGER EMPLOYED BY YOUR ORGANIZATION.

UNCLASSIFIED
SECURITY CLASSIFICATION OF THIS PAGE

REPORT DOCUMENTATION PAGE

1a REPORT SECURITY CLASSIFICATION UNCLASSIFIED	1b RESTRICTIVE MARKINGS
2a SECURITY CLASSIFICATION AUTHORITY N/A since Unclassified	3 DISTRIBUTION / AVAILABILITY OF REPORT Approved for public release; distribution is unlimited.
2b DECLASSIFICATION / DOWNGRADING SCHEDULE N/A since Unclassified	
4 PERFORMING ORGANIZATION REPORT NUMBER(S) UTRC-926388	5 MONITORING ORGANIZATION REPORT NUMBER(S) DNA-TR-85-156
6a NAME OF PERFORMING ORGANIZATION United Technologies Research Center 6b OFFICE SYMBOL (If applicable)	7a NAME OF MONITORING ORGANIZATION Director Defense Nuclear Agency
6c ADDRESS (City, State, and ZIP Code) 400 Main Street East Hartford, CT 06108	7b ADDRESS (City, State, and ZIP Code) Washington, DC 20305-1000
8a NAME OF FUNDING / SPONSORING ORGANIZATION 8b OFFICE SYMBOL (If applicable)	9 PROCUREMENT INSTRUMENT IDENTIFICATION NUMBER DNA 001-83-C-0044
8c ADDRESS (City, State, and ZIP Code)	10 SOURCE OF FUNDING NUMBERS PROGRAM ELEMENT NO: 62715H; PROJECT NO: S99QMXB; TASK NO: I; WORK UNIT ACCESSION NO: DH008242

11 TITLE (Include Security Classification)
THEORETICAL STUDY OF THE RADIATIVE AND KINETIC PROPERTIES OF SELECTED METAL OXIDES AND AIR MOLECULES

12 PERSONAL AUTHOR(S)
Michels, H. H. and Hobbs, R. H.

13a TYPE OF REPORT	13b TIME COVERED	14 DATE OF REPORT (Year, Month, Day)	15 PAGE COUNT
Technical	FROM 830115 TO 850205	850501	90

16 SUPPLEMENTARY NOTATION
This work was sponsored by the Defense Nuclear Agency under RDT&E RMSS Code B322084466 S99QMXBI00025 H2590D.

17 COSATI CODES			18 SUBJECT TERMS (Continue on reverse if necessary and identify by block number)
FIELD	GROUP	SUB-GROUP	
4	1		UO UO^+ UO_2^+ UO_2
7	5		Potential Energy Curves

19 ABSTRACT (Continue on reverse if necessary and identify by block number)

A theoretical research program directed toward the study of the energetics and LWIR radiative properties of selected uranium/oxygen band systems has been undertaken. Included in this research program was the investigation of the strongest electronic and vibrational bands in the LWIR region for the species UO, UO^+, UO_2, and UO_2^+. The program for accomplishing this research effort was formulated into three separate tasks: a) adaption of our electronic structure codes to the DNA CYBER 176 System, b) calculation of pertinent electronic wavefunctions and energies, as a function of internuclear separation within a relativistic framework, for selected species of the uranium/oxygen system which may be important in the LWIR region, and c) calculation of electronic transition moments and transition probabilities between specific vibrational levels of the electronic states corresponding to the strongest radiating band systems belonging to the uranium/oxygen system and prediction of IR and possible optical oscillator strengths.

Our calculations indicated that the species UO^+ will be efficiently solar pumped and

20 DISTRIBUTION / AVAILABILITY OF ABSTRACT	21 ABSTRACT SECURITY CLASSIFICATION
☐ UNCLASSIFIED/UNLIMITED ☒ SAME AS RPT ☐ DTIC USERS	UNCLASSIFIED
22a NAME OF RESPONSIBLE INDIVIDUAL Betty L. Fox	22b TELEPHONE (Include Area Code) (202) 325-7042
	22c OFFICE SYMBOL DNA/STTI

DD FORM 1473, 84 MAR 83 APR edition may be used until exhausted
All other editions are obsolete

SECURITY CLASSIFICATION OF THIS PAGE
UNCLASSIFIED

19. ABSTRACT (Continued)

will exhibit strong absorption/radiation in the region $0.6 \lesssim \lambda \lesssim 11.3\ \mu$. Further, we predict efficient conversion of solar photons to IR photons for this species. For UO_2^+, a careful re-evaluation of the ground and low-lying electronic states indicates that the $^2\Delta_g$ state, lying at ~ 33000 cm^{-1} is the first strongly optically connected state. The wavelength for excitation of this and higher coupled electronically excited states is λ <300 nm, which places them beyond the main region of the solar flux. The neutral UO_2 species has the first strongly coupled optical transition at λ ~ 2.60 nm, again beyond the region for efficient solar pumping. The pathways for conversion of solar photons to the LWIR region are still uncertain but strong LWIR radiation (f_{01} ~ 1.2 x 10^{-4}) is predicted for the vibrational transitions of the ground $^2\Phi_u$ state of UO_2^+. Further studies of UO_2^+, an examination of the doubly ionized species (U^{++}, UO^{++}, UO_2^{++}), and an analysis of the relative importance of dielectronic recombination in this system are indicated.

Keywords: Potential Energy Curves; Excitation; dielectronic recombination; Coupling; Interac

SUMMARY

A theoretical research program directed toward the study of the energetics and LWIR radiative properties of selected uranium/oxygen band systems has been undertaken. Included in this research program was the investigation of the strongest electronic and vibrational bands in the LWIR region for the species UO, UO^+, UO_2, UO_2^+, and UO_2^{++}. The program for accomplishing this research effort was formulated into three separate tasks: a) adaption of our electronic structure codes to the DNA CYBER 176 System, b) calculation of pertinent electronic wavefunctions and energies, as a function of internuclear separation and within a relativistic framework, for selected species of the uranium/oxygen system which may be important in the LWIR region, and c) calculation of electronic transition moments and transition probabilities between specific vibrational levels of the electronic states corresponding to the strongest radiating band systems belonging to the uranium/oxygen system and prediction of IR and possible optical oscillator strengths.

Our calculations indicate that the species UO^+ will be efficiently solar pumped and will exhibit strong absorption/radiation in the region $0.6 \lesssim \lambda \lesssim 11.3$ μ. Further, we predict efficient conversion of solar photons to IR photons for this species. For UO_2^+, a careful re-evaluation of the ground and low-lying electronic states indicates that the $^2\Delta_g$ state, lying at ~ 33000 cm^{-1} is the first strongly optically connected state. The wavelength for excitation of this and higher coupled electronically excited states is $\lambda < 300$ nm, which places them beyond the main region of the solar flux. The neutral UO_2 species has the first strongly coupled optical transition at $\lambda \sim 2.60$ nm, again beyond the region for efficient solar pumping. The pathways for conversion of solar photons to the LWIR region are still uncertain but strong LWIR radiation ($f_{01} \sim 1.2 \times 10^{-4}$) is predicted for the vibrational transitions of the ground $^2\Phi_u$ state of UO_2^+. Further studies of UO_2^+, an examination of the doubly ionized species (U^{++}, UO^{++}, UO_2^{++}), and an analysis of the relative importance of dielectronic recombination in this system are indicated.

PREFACE

This report was prepared by the United Technologies Research Center, East Hartford, Connecticut, under Contract DNA 001-83-C-0044. The research was performed under Program Element 62715H, Project S99QMXB, Task Area I, Work Unit 00025 and was funded by the Defense Nuclear Agency (DNA).

Inclusive dates of research were 1983 January 15 through 1985 March 2. Dr. Kenneth Schwartz (RAAE) was the Contract Technical Manager (CTM) for this contract.

Very useful discussions with Drs. Russell Armstrong (Air Force Geophysics Lab), Morris Krauss (National Bureau of Standards), Robert Field (MIT), Douglas Archer (Mission Research Corporation), Forrest Gilmore (R&D Associates) and G. A. Peterson (UTRC) are also acknowledged.

All aspects of the research work reported herein were aided by the skilled help of Judith B. Addison (UTRC), who carried out much of the computer program development and assisted in the analysis of the calculated data and in the preparation of this final report.

Conversion Table

(Conversion factors for U. S. customary to metric (SI) units of measurement)

To Convert From	To	Multiply By
angstrom	meters (m)	1.000 000 X E -10
atmosphere (normal)	kilo pascal (kPa)	1.013 25 X E +2
bar	kilo pascal (kPa)	1.000 000 X E +2
barn	meter^2 (m^2)	1.000 000 X E -28
British thermal unit (thermochemical)	joule (J)	1.054 350 X E +3
cal (thermochemical)/cm^2	mega joule/m^2(MJ/m^2)	4.184 000 X E -2
calorie (thermochemical)	joule (J)	4.184 000
calorie (thermochemical)/g	joule per kilogram (J/kg)	4.184 000 X E +3
curie	giga becquerél (GBq)	3.700 000 X E +1
degree Celsius	degree kelvin (K)	$t = t°_C + 273.15$
degree (angle)	radian (rad)	1.745 329 X E-2
degree Fahrenheit	degree kelvin (K)	$t = (t°_F + 459.67)/1.8$
electron volt	joule (J)	1.602 19 X E -19
erg	joule (J)	1.000 000 X E -7
erg/second	watt (W)	1.000 000 X E -7
foot	meter (m)	3.048 000 X -1
foot-pound-force	joule (J)	1.355 818
gallon (U.S. liquid)	meter^3 (m^3)	3.785 412 X E -3
inch	meter (m)	2.540 000 X E-2
jerk	joule (J)	1.000 000 X E +9
joule/kilogram (J/kg) (radiation dose absorbed)	gray (Gy)	1.000 000
kilotons	terajoules	4.183
kip (1000 lbf)	newton (N)	4.448 222 X E +3
kip/inch^2 (ksi)	kilo pascal (kPa)	6.894 757 X E +3
ktap	newton-second/m^2 ($N-s/m^2$)	1.000 000 X E +2
micron	meter (m)	1.000 000 X E -6
mil	meter (m)	2.540 000 X -5

Conversion Table (Concluded)

To Convert From	To	Multiply By
mile (international)	meter (m)	1.609 344 X E +3
ounce	kilogram (kg)	2.834 952 X E -2
pound-force (lbf avoirdupois)	newton (N)	4.448 222
pound-force inch	newton-meter (N•m)	1.129 848 X E -1
pound-force/inch	newton/meter (N/m)	1.751 268 X E +2
pound-force/foot^2	kilo pascal (kPa)	4.788 026 X E -2
pound-force/inch^2 (psi)	kilo pascal (kPa)	6.894 757
pound-mass (lbm avoirdupois)	kilogram (kg)	4.535 924 X E -1
pound-mass-foot^2 (moment of inertia)	kilogram-meter^2 (kg•m^2)	4.214 011 X E -2
pound-mass/foot^3	kilogram-meter^3 (kg/m^3)	1.601 846 X E +1
rad (radiation dose absorbed)	gray (Gy)	1.000 000 X E -2
roentgen	coulomb/kilogram (C/kg)	2.579 760 X E -4
shake	second (s)	1.000 000 X E -8
slug	kilogram (kg)	1.459 390 X E +1
torr (mm Hg, 0°C)	kilo pascal (kPa)	1.333 22 X E -1

TABLE OF CONTENTS

LIST OF TABLES

SECTION 1

INTRODUCTION

The release of certain chemical species into the upper atmosphere results in luminous clouds that display the resonance electronic-vibration-rotation spectra of the chemically reacting species. Such spectra are seen in rocket releases of chemicals for upper atmospheric studies, upon re-entry into the atmosphere of artificial satellites and missiles, and as a result of energy deposition in the atmosphere caused by nuclear weapons effects. Of particular interest in this connection is the observed spectra of certain metallic oxides. From band intensity distributions of the spectra, and knowledge of the f-values for electronic and vibrational transitions, the local conditions of the atmosphere can be determined (Reference 1). Such data are fundamental for the analysis of detection and discrimination problems.

Present theoretical efforts, which are directed toward a more complete and realistic analysis of the transport equations governing atmospheric relaxation and the propagation of artificial disturbances, require detailed information of thermal opacities and LWIR absorption in region of temperature and pressure where both atomic and molecular effects are important (References 2 and 3). Although various experimental techniques have been employed for both atomic and molecular systems, theoretical studies have been largely confined to an analysis of the properties (bound-bound, bound-free and free-free) of atomic systems (References 4 and 5). This has been due in large part to the unavailability of reliable wavefunctions for diatomic molecular systems, and particularly for excited states or states of open-shell structure. Only recently (References 6-8) have reliable procedures been prescribed for such systems which have resulted in the development of practical computational programs.

The application of these computational methods to studies of the electronic structure and radiation characteristics of metal oxides has been reported for several of the lighter systems (References 9-11). A preliminary study of the uranium/oxygen system has been reported by Michels (Reference 12) which identified a large number of low-lying molecular states for both the

UO and UO^+ systems. Of particular interest was the discovery of two structures for UO^+ that resulted from two different spin-couplings of the uranium valence electrons. These results suggested strong LWIR radiation in UO^+ arising from different electronic state transitions.

An inherent uncertainty in these preliminary calculations was present, owing to the neglect of relativistic effects that were much too difficult to include in molecular calculations at that period of time. The 7s valence electron of uranium, and its corresponding σ-bonding molecular orbital, are highly relativistic in nature which results in a contracted charge density relative to that which would occur in lighter molecular systems. The effect of this contraction on the relative positions of the low-lying electronic states of the uranium/oxygen system can now be calculated with some degree of confidence using newly developed relativistic computer codes.

Because of inherent difficulties in the experimental determination of the spectroscopy, transition probabilities and LWIR radiation for metal oxide systems and in light of the aforementioned recent progress in the calculation of relativistic electronic wavefunctions, especially for diatomic systems, a technical program for calculating these properties was undertaken for the Defense Nuclear Agency under Contract DNA001-82-C-0015. The emphasis in this work was on the ions of uranium and uranium oxide (U^+, UO^+) since these have been determined to be important radiators in the LWIR region. These studies indicated that UO_2^+ and the doubly ionized species, U^{++}, UO^{++} and UO_2^{++}, should also be considered because of their role in charge neutralization processes and their potential as early-time radiators.

A careful re-evaluation of the ground and low-lying excited states of UO_2^+ was carried out under the current research program. Earlier studies have suggested the possibility of strong absorption for this species in the solar pumped wavelength region. More definitive studies which rule against this possibility are presented in this report.

The general composition of this report is as follows. In Section II, we present a description of the mathematical methods which were employed in this research. Included in Section II are sub-sections which deal with the construction of electronic wavefunctions, the calculations of expectation

properties, the evaluation of molecular transition probabilities, and the calculation of electronic wavefunctions using both the ab initio and density functional methods. This is followed by Section III which describes the inclusion of relativistic effects into the density functional (X_α) method. The calculated results and pertinent discussion are presented in Section IV. Recommendations are presented in Section V.

SECTION 2

METHOD OF APPROACH - NONRELATIVISTIC METHODS

2.1 QUANTUM MECHANICAL CALCULATIONS

Central to these theoretical studies are the actual quantum-mechanical calculations which must be carried out for the atomic and molecular species. For added clarity, various aspects of these calculations are discussed in individual subsections.

2.1.1 Levels of Approximation

Much evidence on diatomic and polyatomic systems indicates the inadequacy of a minimum Slater-type-orbital (STO) basis for constructing quantitatively correct molecular wavefunctions (References 13 and 14). This means inner-shell and valence-shell STO's of quantum numbers appropriate to the atoms (1s, 2s, 2p, for C, N, O; etc.). The main deficiency of the minimum basis set is in its inability to properly describe polarization and the change of orbital shape for systems which exhibit large charge transfer effects. Values of the screening parameters ζ for each orbital can either be set from atomic studies or optimized in the molecule; the latter approach is indicated for studies of higher precision. When high chemical accuracy is required, as for the detailed studies of the ground or a particular excited state of a system, a more extended basis must be used. Double-zeta plus polarization functions or optimized MO's are required for reliable calculated results of chemical accuracy.

The chosen basis sets give good results only when used in a maximally flexible manner. This implies the construction of CI wavefunctions with all kinds of possible orbital occupancies, so that the correlation of electrons into overall states can adjust to an optimum form at each geometrical conformation and for each state. Except when well-defined pairings exist, as for closed shell and exchange dominated systems, a single-configuration study (even of Hartree-Fock quality) will be inadequate.

2.1.2 Spin and Symmetry

Proper electronic states for systems composed of light atoms should possess definite eigenvalues of the spin operator S^2 as well as an appropriate geometrical symmetry. The geometrical symmetry can be controlled by the assignment of orbitals to each configuration, but the spin state must be

obtained by a constructive or projective technique. Formulas have been developed (Reference 15) for projected construction of spin states from orthogonal orbitals, and programs implementing these formulas have been in routine use at UTRC for several years.

One of the least widely appreciated aspects of the spin-projection problem is that the same set of occupied spatial orbitals can sometimes be coupled to give more than one overall state of given S quantum number. It is necessary to include in calculations all such spin couplings, as the optimum coupling will continuously change with changes in the molecular conformation. This is especially important in describing degenerate or near-degenerate excited electronic states.

2.1.3 Method of Ab Initio Calculation

A spin-free, nonrelativistic, electrostatic Hamiltonian is employed in the Born-Oppenheimer approximation. In systems containing atoms as heavy as Kr, this approximation is quite good for low-lying molecular states. For a diatomic molecule containing n electrons, the approximation leads to an electrostatic Hamiltonian depending parametrically on the internuclear separation, R:

$$\mathcal{H}(R) = -\frac{1}{2}\sum_{i=1}^{n}\nabla_i^2 - \sum_{i=1}^{n}\frac{Z_A}{r_{iA}} - \sum_{i=1}^{n}\frac{Z_B}{r_{iB}} + \frac{Z_A Z_B}{R} + \sum_{i>j\geq 1}^{n}\frac{1}{r_{ij}} \qquad (1)$$

where Z_A and Z_B are the charges of nuclei A and B, and r_{iA} is the separation of electron i and nucleus A. $\mathcal{H}$ is in atomic units (energy in hartrees, length in bohrs).

Electronic wavefunctions $\Psi(R)$ are made to be optimum approximations to solutions, for a given R, of the Schrodinger equation

$$\mathcal{H}(R)\Psi(R) = E(R)\Psi(R) \qquad (2)$$

by invoking the variational principle

$$\delta W(R) = \delta \frac{\int \Psi^*(R)\mathcal{H}(R)\Psi(R)\,d\tau}{\int \Psi^*(R)\Psi(R)\,d\tau} \qquad (3)$$

The integrations in Equation (3) are over all electronic coordinates and the stationary values of W(R) are approximations to the energies of states described by the corresponding $\psi(R)$. States of a particular symmetry are studied by restricting the electronic wavefunction to be a projection of the appropriate angular momentum and spin operators. Excited electronic states corresponding to a particular symmetry are handled by construction of configuration-interaction wavefunctions of appropriate size and form.

The specific form for $\psi(R)$ may be written

$$\Psi(R) = \sum_{\mu} c_{\mu} \Psi_{\mu}(R) \tag{4}$$

where each $\psi_{\mu}(R)$ is referred to as a configuration, and has the general structure

$$\Psi_{\mu}(R) = \mathcal{A} \mathcal{O}_S \prod_{i=1}^{n} \Psi_{\mu i}(\underset{\sim}{r}_i, R)\, \theta_M \tag{5}$$

where each $\phi_{\mu i}$ is a spatial orbital, $\mathcal{A}$ is the antisymmetrizing operator, $\mathcal{O}_s$ is the spin-projection operator for spin quantum number S, and θ_M is a product of α and β one-electron spin functions of magnetic quantum number M. No requirement is imposed as to the double occupancy of the spatial orbital, so Equations (4) and (5) can describe a completely general wavefunction.

In Hartree-Fock calculations $\psi(R)$ is restricted to a single ψ_{μ} which is assumed to consist as nearly as possible of doubly-occupied orbitals. The orbitals $\phi_{\mu i}$ are then selected to be the linear combinations of basis orbitals best satisfying Equation (3). Writing

$$\phi_{\mu i} = \sum_{\nu} a_{\nu i} \chi_{\nu} \tag{6}$$

the $a_{\nu i}$ are determined by solving the matrix Hartree-Fock equations

$$\sum_{\nu} F_{\lambda \nu} a_{\nu i} = \epsilon_i \sum_{\nu} S_{\lambda \nu} a_{\nu i} \quad \text{(each } \lambda\text{)} \tag{7}$$

where ε_i is the <u>orbital</u> energy of $\phi_{\mu i}$.

The Fock operator $F_{\lambda\nu}$ has been thoroughly discussed in the literature (Reference 16) and depends upon one- and two-electron molecular integrals and upon the $a_{\nu i}$. This makes Equation (7) nonlinear and it is therefore solved iteratively. UTRC has developed programs for solving Equation (7) for both closed and open-shell systems, using basis sets consisting of Slater-type atomic orbitals. Examples of their use are in the literature (Reference 7).

In configuration interaction calculations, the summation of Equation (4) has more than one term, and the $\underset{\sim}{c}_{\mu}$ are determined by imposing Equation (3) to obtain the secular equation

$$\sum_{\nu} (H_{\mu\nu} - w s_{\mu\nu}) c_{\nu} = 0 \qquad (\text{each } \mu) \tag{8}$$

where

$$H_{\mu\nu} = \int \Psi_{\mu}^{*}(R)\, \mathcal{H}(R)\, \Psi_{\nu}(R)\, d\tau$$

$$S_{\mu\nu} = \int \Psi_{\mu}^{*}(R)\, \Psi_{\nu}(R)\, d\tau \tag{9}$$

Equation (8) is solved by matrix diagonalization using either a modified Givens method (Reference 17) or a method due to Shavitt (Reference 18).

The matrix elements $H_{\mu\nu}$ and $S_{\mu\nu}$ may be reduced by appropriate operator algebra to the forms

$$H_{\mu\nu} = \sum_{P} \epsilon_P \left\langle \theta_M \middle| \mathcal{O}_S P \middle| \theta_M \right\rangle \left\langle \prod_{i=1}^{n} \Psi_{\mu i}(\underset{\sim}{r}_i, R) \middle| \mathcal{H}(R) P \middle| \prod_{i=1}^{n} \Psi_{\nu i}(\underset{\sim}{r}_i, R) \right\rangle \tag{10}$$

$$S_{\mu\nu} = \sum_{P} \epsilon_P \left\langle \theta_M \middle| \mathcal{O}_S P \middle| \theta_M \right\rangle \left\langle \prod_{i=1}^{n} \Psi_{\mu i}(\underset{\sim}{r}_i, R) \middle| P \middle| \prod_{i=1}^{n} \Psi_{\nu i}(\underset{\sim}{r}_i, R) \right\rangle \tag{11}$$

where P is a permutation and ϵ_p its parity. The sum is over all permutations. $\langle \theta_M | {}_s P | \theta_M \rangle$ is a "Sanibel coefficient" and the remaining factors are spatial integrals which can be factored into one- and two-electron integrals. If the $\phi_{\mu i}$ are orthonormal, Equations (10) and (11) become more tractable and the $H_{\mu\nu}$ and $S_{\mu\nu}$ may be evaluated by explicit methods given in the literature

(Reference 15). Computer programs have been developed for carrying out this procedure, and they have been used for problems containing up to 106 total electrons, 10 unpaired electrons, and several thousand configurations.

The CI studies described above can be carried out for any orthonormal set of $\phi_{\mu i}$ for which the molecular integrals can be calculated. Programs developed by UTRC make specific provision for the choice of the $\phi_{\mu i}$ as Slater-type atomic orbitals, as symmetry molecular orbitals, as Hartree-Fock orbitals, or as more arbitrary combinations of atomic orbitals.

2.1.4 Molecular Integrals

The one- and two-electron integrals needed for the above described method of calculation are evaluated for STO's by methods developed by the present investigators (Reference 19). All needed computer programs have been developed and fully tested at UTRC.

2.1.5 Configuration Selection

Using a minimum basis plus polarization set of one-electron functions, a typical system can have of the order of 10^4 configurations in full CI (that resulting from all possible orbital occupancies). It is therefore essential to identify and use the configurations describing the significant part of the wavefunction. There are several ways to accomplish this objective. First, one may screen atomic-orbital occupancies to eliminate configurations with excessive numbers of anti-bonding orbitals. A third possibility is to carry out an initial screening of configurations, rejecting those whose diagonal energies and interaction matrix elements do not satisfy significance criteria. Programs to sort configurations on all the above criteria are available at UTRC.

Other, potentially more elegant methods of configuration choice involve formal approaches based on natural-orbital (Reference 20) or multiconfiguration SCF (Reference 21) concepts. To implement the natural-orbital approach, an initial limited-CI wavefunction is transformed to natural-orbital form, and the resulting natural orbitals are used to form a new CI. The hoped-for result is a concentration of the bulk of the CI wavefunction into a smaller number of significant terms. The multiconfiguration SCF approach is more cumbersome, but in principle more effective. It yields the optimum orbital choice for a preselected set of configurations. This approach works well when a small number of dominant configurations can be readily identified.

It should be emphasized that the problem of configuration choice is not trivial, and represents an area of detailed study in this research. The existence of this problem causes integral evaluation to be far from a unique limiting factor in the work.

2.1.6 Density Function Approach - Xα Model

The Xα model (Reference 22) for the electronic structure of atoms, molecules, clusters and solids is a local potential model obtained by making a simple approximation to the exchange - correlation energy. If we assume a nonrelativistic Hamiltonian with only electrostatic interactions, it can be shown that the total energy E of a system can be written exactly (Reference 23) (in atomic units) as

$$E = \sum_i n_i \left\langle u_i \left| -\tfrac{1}{2}\nabla_i^2 + \sum_\mu \frac{*\mu}{r_{1\mu}} \right| u_i \right\rangle + \tfrac{1}{2} \sum_{\mu \neq \nu} \frac{*\mu *\nu}{r_{\mu\nu}}$$

$$+ \tfrac{1}{2} \sum_{ij} n_i n_j \left\langle u_i u_j \left| \frac{1}{r_{12}} \right| u_i u_j \right\rangle + E_{xc} \qquad (12)$$

This expression is exact provided the u_i are natural orbitals and n_i are their occupation numbers (i.e., eigenfunctions and eigenvalues of the first order density matrix). The first term in Equation (12) represents the kinetic and electron-nuclear energies. The second term is the nuclear repulsion energy. The sums (μ,ν) are over all the nuclear charges in the system. The third term is the electron-electron repulsion term, which represents the classical electrostatic energy of the charge density ρ interacting with itself, where

$$\rho(1) = \sum_i n_i u_i^*(1)\, u_i(1) \qquad (13)$$

The last term E_{xc} represents the exchange correlation energy and can be expressed formally as

$$E_{xc} = \tfrac{1}{2} \int \rho(1)\, d\vec{r}_1 \int \frac{\rho_{xc}(1,2)}{r_{12}}\, d\vec{r}_2 \,, \qquad (14)$$

where $\rho_{xc}(1, 2)$ represents the exchange-correlation hole around an electron at position 1. In the exact expression, ρ_{xc} is dependent on the

second-order density matrix. In the Hartree-Fock approximation E_{xc} is the exchange energy, ρ_{xc} represents the Fermi hole due to the exclusion principle and depends only on the first-order density matrix. In the Xα method, we make a simpler assumption about ρ_{xc}. If we assume that the exchange-correlation hole is centered on the electron and is spherically symmetric, it can be shown that the exchange-correlation potential

$$U_{xc} = \int \frac{\rho_{xc}(1,2)}{r_{12}} \, d\vec{r}_2 \tag{15}$$

is inversely proportional to the range of the hole, r_s, where r_s is defined by

$$\frac{4\pi}{3} \, r_s^3 \, \rho(1) = 1 \tag{16}$$

Therefore, in the Xα model, the potential U_{xc} is proportional to $\rho^{1/3}(\vec{r})$. We define a scaling parameter α such that

$$U_{x\alpha}(1) = -\frac{9\alpha}{2} \left(3\rho(1)/8\pi\right)^{1/3} \tag{17}$$

The expression in Equation (37) is defined so that $\alpha = 2/3$ for the case of a free electron gas in the Hartree-Fock model (Reference 24) and $\alpha = 1$ for the potential originally suggested by Slater (Reference 25). A convenient way to choose this parameter for molecular and solid state applications is to optimize the solutions to the Xα equations in the atomic limit. Schwarz (Reference 26) has done this for atoms from z = 1 to z = 41 and found values between 2/3 and 1.

In the "spin polarized" version of the Xα theory, it is assumed (as in the spin-unrestricted Hartree-Fock model) that electrons interact only with a potential determined by the charge density of the same spin. In this case the contribution to the total energy is summed over the two spins, $s = \pm 1/2$.

$$E_{xc} = \frac{1}{2} \sum_s \int \rho_s(1) \, U_{x\alpha,s}(1) \, d\vec{r}_1 \tag{18}$$

where the potential is spin-dependent

$$U_{X\alpha,S}(1) = -\frac{9\alpha}{2}\left(3\rho_S(1)/4\pi\right)^{1/3} \tag{19}$$

and ρ_s is the charge density corresponding to electrons of spin s. The spin polarized Xα model is useful for describing atoms and molecules with open-shell configurations and crystals which are ferromagnetic or antiferromagnetic.

Once one has made the Xα approximation to the total energy functional E in Equation (12), then the rest of the theory follows from the application of the variational principle. The orbitals u_i are determined by demanding that E be stationary with respect to variations in u_i. This leads to the set of one-electron Xα equations

$$\left[-\frac{1}{2}\nabla_1^2 + \sum_{\mu}\frac{Z_\mu}{r_{1\mu}} + \int\frac{\rho(2)}{r_{12}}d\vec{r}_2 + \frac{2}{3}U_{X\alpha}\right]u_i = \epsilon_i u_i \tag{20}$$

where ε_i is the one-electron eigenvalue associated with u_i. Since $\rho(\vec{r})$ is defined in terms of the orbitals u_i, Equation (20) must be solved iteratively, until self-consistency is achieved. Empirically, if one takes as an initial guess that ρ is approximately a sum of superimposed atomic charge densities, then the convergence of this procedure is fairly rapid. The factor of 2/3 multiplying the potential is a result of the linear dependence of E_{xc} on ρ. This also has a consequence that the Xα eigenvalues ε_i do not satisfy Koopman's theorem, i.e., they cannot be interpreted as ionization energies. However, it can be shown that the ε_i are partial derivatives of the total expression of Equation (12) with respect to the occupation number,

$$\epsilon_i = \frac{\partial E}{\partial n_i} \tag{21}$$

If E were a linear function of n_i, then Koopmans' theorem would hold. However, because of the dominant Coulomb term, E is better approximated by a quadratic function in n_i. This leads to the "transition state" approximation which allows one to equate the difference in total energy between the state (n_i, n_j) and $(n_i - 1, n_j + 1)$ to the difference in the one-electron energies $\varepsilon_j - \varepsilon_i$ calculated in the state $(n_i - 1/2, n_j + 1/2)$. The error in this approximation is proportional to third-order derivatives of E with respect to n_i and n_j, which are usually small (Reference 27). The main advantage of using the transition state rather than directly comparing the total energy values is computational convenience, especially if the total energies are large numbers and the difference is small.

The relationship of Equation (21) also implies the existence of a "Fermi level" for the ground state. This can be seen by varying E with respect to n_i under the condition that the sum $\sum_i n_i$ is a constant, i.e.,

$$\delta\left[E - \lambda \sum_i n_i\right] = 0 \tag{22}$$

implies $\partial E / \partial n_i = \lambda$, where λ is a Lagrangian multiplier. This implies that the total energy is stationary when all the one-electron energies are equal. However, the occupation numbers are also subject to the restriction $0 \leq n_i \leq 1$. This leads to the following conditions on the ground state occupation numbers;

$$\begin{aligned} \epsilon_i < \lambda &: \; n_i = 1 \\ \epsilon_i > \lambda &: \; n_i = 0 \\ \epsilon_i = \lambda &: \; 0 \leq n_i \leq 1 \end{aligned} \tag{23}$$

In other words, the ground state eigenvalues obey Fermi statistics with λ representing the Fermi energy. It should be noted that, in contrast to the Hartree-Fock theory, where all the n_i are either 0 or 1, the Xα model predicts, in some cases, fractional occupation numbers at the Fermi level. In particular, this will occur in a system (such as transition metal or actinide atom) which has more than one open shell.

The Xα model differs in other significant ways from the Hartree-Fock method. In fact, the simplification introduced in approximating the total energy expression introduces several distinct advantages over Hartree-Fock:

1. The primary advantage is purely computational. The one-electron potential in Equation (20) is orbital-independent and local, i.e., it is the same for all electrons (except in the spin-polarized Xα theory) and is a multiplicative operator. On the other hand, the Hartree-Fock potential is nonlocal, or equivalently, there is a different local potential for each orbital. This involves a great deal more computational effort, especially for systems described by a large number of orbitals. It has been shown (Reference 28) that the Xα orbitals for the first and second row atoms are at least as accurate as a double-zeta basis set, and are probably better for larger atoms which involve electrons with $\ell \geq 2$.

2. The orbital-independent Xα potential leads to a better one-electron description of electronic excitations of a system. Both the unoccupied ($n_i = 0$) and occupied ($n_i = 1$) eigenfunctions are under the influence of the same potential resulting from the other N-1 electrons. The Hartree-Fock virtual orbitals see a potential characteristic of the N occupied orbitals, and therefore are not as suitable for describing the excited states. Actually, although the ground state virtual eigenvalues are usually a good description of the one-electron excitations, the virtual spectrum of the transition state potential where one-half an electron has been removed from the system gives a much better first-order picture of these levels (Reference 29).

3. As has been shown by Slater (Reference 30), the Xα model rigorously satisfies both the virtual and Hellman-Feynman theorems, independent of the value of the parameter α. This is convenient for calculating the force on a nucleus directly in terms of a three-dimensional integral, rather than the six-dimensional integrals in the expression for the total energy of Equation (12).

2.1.7 Computational Aspects of the Xα Method

In application of the Xα model to finite molecular systems, there are two practical aspects of the calculations which must be considered. The first

concerns the choice of the integration framework for describing the molecular wavefunctions and the second deals with the choice of the exchange parameter, α, in different regions of space.

In computations with heteronuclear molecules, there are several free parameters that must be chosen: the ratio of sphere radii for the atomic spheres of integration at a given internuclear separation, the degree of sphere overlap, and the value of the exchange parameter in the atomic spheres and the intersphere region.

It has been found that changing the ratio of the sphere radii for the two atoms in a heteronuclear diatomic molecule introduces changes in the total energy that can be large on a chemical scale ($\sim$ 1 eV). A choice for sphere radii based on covalent bonding radii does not necessarily provide a good estimate for these calculations. The value of the exchange parameter, α, and the sphere radii and/or sphere overlap is normally fixed in Xα calculations for crystals where the geometry is fixed. However, to develop a potential curve, the molecule description needs to change substantially as the internuclear separation varies and the changing sphere radii include varying fractions of the total molecular charge (Reference 31). Studies made at UTRC have shown that at any given separation the total energy calculated from the Xα model is a minimum at the radii ratio where the spherically averaged potentials from the two atomic centers is equal at the sphere radius.

$$V_1(r_{s_1}) = V_2(r_{s_2}) \tag{24}$$

This relationship between the potential match at the sphere boundary and the minimum in the total energy appears to hold exactly for "neutral" atoms and holds well for ionic molecular constituents. In the case of two ionic species, the long range tail of the potential must go like +2/R from one ion and -2/R (in Rydbergs) for the other ion and so at large internuclear separations, the tails of the potential cannot match well. However, at reasonable separations, the 1/R character of the potential does not invalidate the potential match criterion for radii selection. This match for the atomic potentials is applied to the self-consistent potentials.

In molecules with significant charge sharing in the bonds, the radii of the atomic spheres is frequently increased in Xα calculations so that an overlap region appears in the vicinity of the bond (Reference 32). Studies made at UTRC show that the contribution to the total molecular energy from the exchange integral shows a minimum at the optimum sphere radius or sphere overlap. This provides a sensitive criterion for selecting these parameters.

The values of the exchange parameters in the spherical integration region around each atomic center are frequently set at the atomic values both for neutral and for ionic molecular constituents. However, for light atoms, the value of α which best reproduces Hartree-Fock results varies substantially with ionicity. In argon, the following table compares, for the neutral atom and the positive ion, the HF energy and the Xα energy calculated for several values of α.

	α	Xα Energy	HF Energy
Ar^0	.72177	526.8176	526.8173
$Ar^{+1/2}$	.72177	526.5857	-
	.72213	526.6007	-
Ar^{+1}	.72177	526.2447	-
	.72213	526.2596	-
	.72249	526.2745	526.2743

The optimum value of α changes even more rapidly in the fluorine atom going from 0.73732 for F^0 to .72991 for F^{-1}. Since the total energy depends linearly on α, this parameter must be chosen carefully.

The intersphere exchange coefficient is chosen to be a weighted average of the atomic exchange parameters from the two constituents. At small internuclear separations, the optimum radius for an atomic sphere frequently places significant amounts of charge outside that atomic sphere - charge that is still strongly associated with its original center rather than being transferred to the other center or associated with the molecular binding region. To best account for these cases the weighting coefficients are chosen to reflect the origin of the charge in the intersphere (or outersphere region),

$$\alpha_{\text{intersphere}} = \frac{\alpha_{s_1}\,(Q_{s_1} - Q_1^{\circ}) + \alpha_{s_2}\,(Q_{s_2} - Q_2^{\circ})}{(Q_{s_1} - Q_1^{\circ}) + (Q_{s_2} - Q_2^{\circ})} \tag{25}$$

where $(Q_{s_i} - Q_i^{\circ})$ is the charge lost from sphere i relative to its atomic value (or ionic value) Q_i° and α_{s_i} is the atomic exchange parameter for sphere i. This value for $\alpha_{\text{intersphere}}$ is calculated dynamically - it is updated after each iteration in the self-consistent calculation.

While for heavy atoms, these changes in the exchange parameter would be small, the α's for small atoms vary rapidly with z (and with ionicity). The correct choice of the exchange parameters influences not only the total energy calculated for the molecule but also in some cases affects the distribution of charge between the atomic spheres and the intersphere region.

2.2 TRANSITION PROBABILITIES

The electronic and vibrational-rotational wavefunctions of a pair of states can be used to calculate transition probabilities. If two molecular states are separated in energy by an amount $\Delta E_{nm} = hc\nu$ (h = Planck's constant, c = velocity of light, ν = frequency in wave numbers), the semi-classical theory of radiation (References 33 and 34) yields for the probability of a spontaneous transition from an upper state n to a lower state m

$$A_{nm} = \frac{4}{3} \frac{\Delta E_{nm}^3}{\hbar^4 c^3} \frac{S_{nm}}{g_n} \tag{26}$$

Here A_{nm} is the Einstein coefficient for spontaneous transition from level n → m, g_n is the total degeneracy factor for the upper state

$$g_n = (2 - \delta_{\sigma,\Lambda'})(2S' + 1)(2J' + 1) \tag{27}$$

and S_{nm} is the total strength of a component line in a specific state of polarization and propagated in a fixed direction. A related quantity is the mean radiative lifetime of state n defined by

$$\frac{1}{\tau_n} = \sum_{m<n} A_{nm} \tag{28}$$

the summation being over all lower levels which offer allowed connections. The intensity of the emitted radiation is

$$I_{nm} = \Delta E_{nm} N_n A_{nm} \tag{29}$$

where N_n is the number density in the upper state n. This analysis assumes that all degenerate states at the same level n are equally populated, which will be true for isotropic excitation. The total line strength S_{nm} can be written as the square of the transition moment summed over all degenerate components of the molecular states n and m:

$$S_{nm} = \sum_{i,j} \left| M_{ji} \right|^2 \tag{30}$$

where j and i refer to all quantum numbers associated collectively with upper and lower electronic states, respectively.

In the Born-Oppenheimer approximation, assuming the separability of electronic and nuclear motion, the wavefunction for a diatomic molecule can be written as

$$\psi'_{vJM\Lambda} = \psi'_{el}(\underset{\sim}{r}, R)\,\psi_v(R)\,\psi_{JM\Lambda}(\theta, \chi, \phi) \tag{31}$$

where $\psi^i_{el}(\underset{\sim}{r}, R)$ is an electronic wavefunction for state i at fixed internuclear separation R, $\psi_v(R)$ is a vibrational wvefunction for level v and $\psi_{Jn\Lambda}(\theta, x, \phi)$ refers to the rotational state specified by electronic angular momentum Λ, total angular momentum J and magnetic quantum number M. The representation is in a coordinate system related to a space-fixed system by the Eulerian angles (θ, x, ϕ). The transition moment M_{ji} can be written, using the wavefunction given by Equation (31), as

$$M_{ji} = \int \psi^j_{v'J'\Lambda'M'} \left\{ \underset{\sim}{M}^e + \underset{\sim}{M}^n \right\} \psi^j_{v''J''\Lambda''M''}\, d\tau_e d\tau_v d\tau_r \tag{32}$$

The subscripts e, v and r refer to the electronic, vibrational and rotational wavefunctions and $\underset{\sim}{M}^e$ and $\underset{\sim}{M}^n$ are the electronic and nuclear electric dipole moments, respectively. Integration over the electronic wavefunction, in the Born-Oppenheimer approximation, causes the contribution of the nuclear moment M^n to vanish for $i \neq j$. The electronic dipole moment can be written (References 34 and 35) in the form

$$\underset{\sim}{M}^{e} = -\sum_{k} e\underset{\sim}{r}'_{k} = -\left\{\sum_{k} e\underset{\sim}{r}_{k}\right\}\cdot\underset{\sim}{\mathcal{D}}(\theta,\chi,\phi) \tag{33}$$

where the primed coordinates refer to the space fixed system, the coordinates r_k refer to a molecule-fixed system and $\underset{\sim}{\mathcal{D}}(\theta, \chi, \phi)$ is a group rotation tensor whose elements are the direction cosines related to the Eulerian rotation angles (θ, χ, ϕ). Using bracket notation, Equations (32) and (33) can be combined to yield for the transition moment

$$M_{ji} = M^{jv'J'\Lambda'M'}_{iv''J''\Lambda''M''} = \left\langle jv'\left|-\sum_{k} e\underset{\sim}{r}_{k}\right|iv''\right\rangle\cdot\left\langle J'\Lambda'M'\left|\underset{\sim}{\mathcal{D}}(\theta,\chi,\phi)\right|J''\Lambda''M''\right\rangle \tag{34}$$

The matrix elements $\langle J'\ \Lambda'\ M'|\ (\theta, \chi, \phi)|J''\ \Lambda''\ M''\rangle$ determine the group selection rules for an allowed transition and have been evaluated for many types of transitions (References 36-38). Summing Equation (34) over the degenerate magnetic quantum numbers M' and M'' we have from Equation (30)

$$S_{nm} = S^{nv'J'\Lambda'}_{mv''J''\Lambda''} = \mathcal{S}^{J'\Lambda'}_{J''\Lambda''}\, p^{nv'}_{mv''} \tag{35}$$

where $\mathcal{S}^{J'\Lambda'}_{J''\Lambda''}$ is the Hönl-London factor (References 39 and 40)

$$p^{nv'}_{mv''} = \sum_{i,j}\left|\left\langle jv'\left|-\sum_{k} e\underset{\sim}{r}_{k}\right|iv''\right\rangle\right|^{2} \tag{36}$$

is the band strength for the transition. Combining Equations (27), (29) and (35), we have for the intensity of a single emitting line from upper level n:

$$I_{nm} = I^{nv'J'}_{mv''J''} = \frac{4}{3} N_{J'}\,\frac{\left[\Delta E^{nv'J'}_{mv''J''}\right]^{4} S^{nv'J'\Lambda'}_{mv''J''\Lambda''}}{\hbar^{4}c^{3}\omega_{n}(2J'+1)} \tag{37}$$

where $N_{J''}$ is the number density in the upper rotational state J' and $\omega_n = (2-\delta_{\sigma,\Lambda})\ (2S' + 1)$ is the electronic degeneracy. Taking an average value of $E_{m\ v''J''}^{n\ v'J'}$ for the whole band, Equation (37) can be summed to yield the total intensity in the (v', v") band:

$$I_{mv''}^{nv'} = \sum_{J',J''} I_{mv''J''}^{nv'J'} = \frac{4}{3} N_{v'}' \frac{\left[\overline{\Delta E}_{mv''}^{nv'}\right]^4 p_{mv''}^{nv'}}{\hbar^4 c^3 \omega_n} \tag{38}$$

where $N_{v'} = \sum_{J'} N_{j'}$ is the total number density in the upper vibrational level v' and where we make use of the group summation property

$$\sum_{J''} \mathcal{S}_{J''\Lambda''}^{J'\Lambda'} = (2J'+1) \tag{39}$$

Comparing Equations (29) and (38), we have for the Einstein spontaneous transition coefficient of the band (v', v")

$$A_{mv''}^{nv'} = \frac{4}{3} \frac{\left[\Delta E_{mv''}^{nv'}\right]^3 p_{mv''}^{nv'}}{\hbar^4 c^3 \omega_n} \tag{40}$$

Similarly, the lifetime of an upper vibrational level v' of state n can be written

$$\frac{1}{\tau_n} = \sum_{m<n} \sum_{v''} A_{mv''}^{nv'} \tag{41}$$

where the summation runs over all v" for each lower state m. Equation (40) can be cast in the computational form

$$A_{mv''}^{nv'}(\text{sec}^{-1}) = \frac{(21.41759 \times 10^9)}{\omega_n} \left[\Delta E_{mv''}^{nv'}(\text{a.u.})\right]^3 p_{mv''}^{nv'}(\text{a.u.}) \tag{42}$$

where $\Delta E_{m\ v''}^{n\ v'}$ and $p_{m\ v''}^{n\ v'}$ are in atomic units. It is also often convenient to relate the transition probability to the number of dispersion electrons needed to explain the emission strength classically. This number, the f-number or oscillator strength for emission, is given by

$$f_{nm,\,v'v''} = \frac{mc^3h^2}{2e^2\left[\overline{\Delta E}_{mv''}^{nv'}\right]^2} A_{mv''}^{nv'} \tag{43}$$

The inverse process of absorption is related to the above development through the Einstein B coefficient. Corresponding to Equation (29), we have for a single line in absorption

$$\frac{I_{mn}}{I_\nu^0 \Delta x} = \int_{\text{line}\,(v''v'J''J')} K(\nu)\,d\nu = h\nu_{mn} N_m B_{mn} \tag{44}$$

where $K(\nu)$ is the absorption coefficient of a beam of photons of frequency ν and

$$B_{mn} = B_{mv''J''\Lambda''}^{nv'J'\Lambda'} = \frac{2\pi}{3\hbar^2 c} \frac{S_{mv''J''\Lambda''}^{nv'J'\Lambda'}}{\omega_m(2J''+1)} \tag{45}$$

is the Einstein absorption coefficient for a single line. Summing over all lines in the band (v", v'), assuming an average band frequency, we obtain

$$\frac{I_{mv''}^{nv'}}{I_\nu^0 \Delta x} = N_{v''} \frac{2\pi}{3\hbar^2 c\omega_m} p_{mv''}^{nv'} \overline{\Delta E}_{m\nu''}^{n\nu'} \tag{46}$$

where $N_{v''} = \sum_{J''} N_{J''}$ is the total number density in the lower vibrational state v". Corresponding to Equations (42) and (43) we can define an f-number or oscillator strength for absorption as

$$f_{mn,v''v'} = \frac{2m \overline{\Delta E}^{nv'}_{mv''}}{3\hbar^2 e^2 \omega_m} \; p^{nv'}_{mv''} \tag{47}$$

In computational form, Equation (47) becomes

$$f_{mn,v''v'} = \frac{2}{3} \cdot \frac{\overline{\Delta E}^{nv'}_{mv''}(a.u.)}{\omega_m} \; p^{nv'}_{mv''}(a.u.) \tag{48}$$

where $\overline{\Delta E}^{\,n\ v'}_{m\ v''}$ and $p^{n\ v'}_{m\ v''}$ are in atomic units. Combining Equations (40) and (43) and comparing with Equation (47), we see that the absorption and emission f-numbers are related by

$$f_{mn,v''v'} = \left(\frac{\omega_n}{\omega_m}\right) f_{nm,v'\,v''} \tag{49}$$

Some caution must be observed in the use of f-numbers given either by Equation (43) or (47) since both band f-numbers and system f-numbers are defined in the literature. The confusion arises from the several possible band averaging schemes that can be identified.

An integrated absorption coefficient (density corrected) can be defined from Equation (46) as

$$S_{v'',v'} = \frac{1}{P_c} \; I^{nv'}_{mv''} = N_{v''} B_{v'',v'} \left(1 - \exp \frac{-hc\nu_{v'',v'}}{kT}\right) \frac{h\nu_{v'',v'}}{Pc^2} \tag{50}$$

where the exponential factor corrects for stimulated emission. Equation 50 can be written in terms of the absorption f-number as

$$S_{v'',v'} = \frac{\pi e^2}{mc^2} \frac{N_{v''}}{P} \left(1 - \exp \frac{-hc\nu_{v'',v'}}{kT} \right) f_{mn,v''v'} \tag{51}$$

Using h c/k = 1.43880 cm-K°, we obtain a computational formula for the integrated absorption coefficient as $S_{v'',v'}$ ($cm^{-2}.atm^{-1}$) =

$$2.3795 \times 10^7 \left(\frac{273.16}{T(K°)} \right) \left(\frac{N_{v''}}{N_T} \right) \left(1 - \exp \frac{1.43880\, \nu_{v''v'}(cm^{-1})}{T} \right) \cdot f_{mn,v''v'} \tag{52}$$

The total integrated absorption is found from

$$S_{TOTAL} = \sum_{v''} \sum_{v'} S_{v'',v'} \tag{53}$$

where, under normal temperature conditions, only the first few fundamentals and overtones contribute to the summations.

The developments given above are rigorous for band systems where an average band frequency can be meaningfully defined. Further approximations, however, are often made. For example, the electronic component of the dipole transition moment can be defined as

$$R_{ji}(R) = \left\langle j \left| -\sum_k e\underset{\sim}{r}_k \right| i \right\rangle \tag{54}$$

This quantity is often a slowly varying function of R and an average value can sometimes be chosen. Equation (36) can then be written approximately in factored form as

$$p_{mv''}^{nv'} \simeq q_{v'v''} \sum_{i,j} \left| \bar{\mathcal{R}}_{ji}(\bar{R}) \right|^2 \tag{55}$$

where $q_{v'v''}$, the square of the vibrational overlap integral, is called the Franck-Condon factor. $\mathcal{R}_{ji}$ is evaluated at some mean value of the internuclear separation R. In addition, it is sometimes possible to account for a weak R-dependence in $\underset{\sim}{M}^e$ by a Taylor series expansion of this quantity about some reference value, $\mathcal{R}_{\alpha\beta}$, usually referred to the (0, 0) band. We have

$$\mathcal{R}_{ji} \simeq \mathcal{R}_{ji}^{\alpha\beta} \left[1 + a(R - R_{\alpha\beta}) + b(R - R_{\alpha\beta})^2 + \cdots \right] \tag{56}$$

Substituting into Equation (56) and integrating yields

$$p_{mv''}^{nv'} \simeq q_{v'v''} \sum_{i,j} \left| \mathcal{R}_{ji}^{\alpha\beta} \left[1 + a(\overline{R_{v'v''} - R_{\alpha\beta}}) + b(\overline{R_{v'v''} - R_{\alpha\beta}})^2 + \cdots \right] \right|^2 \tag{57}$$

where

$$(\overline{R_{v'v''} - R_{\alpha\beta}}) = \frac{\langle v' | (R - R_{\alpha\beta}) | v'' \rangle}{\langle v' | v'' \rangle} \tag{58}$$

is the R-centroid for the transition and

$$(\overline{R_{v'v''} - R_{\alpha\beta}})^2 = \frac{\langle v' | (R - R_{\alpha\beta})^2 | v'' \rangle}{\langle v' | v'' \rangle} \tag{59}$$

is the R^2-centroid. Note that this last term differs (to second order) from the square of the R-centroid. An alternate procedure can be developed by evaluating Equation (54) at each R-centroid, $\bar{R}_{v'v''}$. Then

$$p^{nv'}_{mv''} \approx q_{v'v''} \sum_{i,j} \left| R_{ji}(R_{v'v''}) \right|^2 \tag{60}$$

Equation (60) assumes that the vibrational wavefunction product $\psi_{v'}$, $\psi_{v''}$, behaves like a delta function upon integration,

$$\psi_{v'} \psi_{v''} = \delta(R - \bar{R}_{v'v''}) \langle v' | v'' \rangle \tag{61}$$

The range of validity of Equation (60) is therefore questionable, particularly for band systems with bad overlap conditions such as oxygen Schumann-Runge. The range of validity of the R-centroid approximation has been examined by Frazer (Reference 41).

The final step in calculating transition probabilities is the determination of $R_{ji}(R)$, the electronic dipole transition moment, for the entire range of internuclear separations, R, reached in the vibrational levels to be considered. This can be expressed in terms of the expansion of Equation (4) as

$$R_{ji}(R) = \sum_{\mu\nu} c^{j*}_{\mu} c^{i}_{\nu} \left\langle \psi_{\mu}(R) \left| \underset{\sim}{M}^{e} \right| \psi_{\nu}(R) \right\rangle \tag{62}$$

where c_{μ}^{j} and c_{ν}^{i} are coefficients for ψ^{j}_{el} and ψ^{i}_{el}, respectively.

An analysis similar to that yielding Equation (10) and (11) gives

$$\left\langle \psi_\mu(R) \left| \underset{\sim}{M}^e \right| \psi_\nu(R) \right\rangle = \sum_p \epsilon_p \left\langle \theta_{M_S} \left| \mathcal{O}_S P \right| \theta_{M_S} \right\rangle \left\langle \prod_{k=1}^{n} \psi_{\mu k}(\underset{\sim}{r}_k, R) \left| \underset{\sim}{M}^e P \right| \prod_{k=1}^{n} \psi_{\nu k}(\underset{\sim}{r}_k, R) \right\rangle \tag{63}$$

The spatial integral in Equation (63) reduces to one-electron integrals equivalent to overlap integrals, and the evaluation of Equation (63) can be carried out by the same computer programs used for Equation (11). Programs for evaluating $_{ji}(R)$ in Equation (62) have been developed at UTRC and examples of their application have appeared in the literature (Reference 8).

For perturbed electronic systems, the transition dipole moment will have a strong R-dependence and R-centroid or other apporximations will be invalid. A direct evaluation of Equation (36) would therefore be required using the fully-coupled system of electronic and vibrational wavefunctions to properly account for the source of the band perturbations.

SECTION 3

DISCUSSION OF RELATIVISTIC METHODS

For heavy atoms ($Z \gtrsim 30$), and molecular systems built from heavy atoms, relativistic effects become increasingly important and should be taken into account in the calculation of the radial wavefunctions. The implementation of relativistic effects into atomic and molecular computer codes is only fairly recent owing to the increased complexities introduced in the self-consistent field (SCF) procedure and the greatly increased computer time required for such calculations. Compared with the non-relativistic case, the Dirac-Hartree-Fock (DHF) method requires that two radial functions, G_{nlj}, corresponding to the large component and F_{nlj}, corresponding to the small component must be calculated for each of the two possible j values. Thus, the numerical work of a DHF relativistic treatment is increased by nearly a factor of four over the nonrelativistic case, exclusive of increased complexities in evaluation of the terms of the Hamiltonian. In view of this, methods that have been developed to date for molecular systems have involved the use of model potentials to represent relativistic effects.

In the calculation of the internal energy of a molecular system comprised of n electrons and N nuclei, and considering only electrostatic interactions between the particles, we have for the total Hamiltonian

$$\mathcal{H} = \mathcal{H}_{el} - \sum \frac{\hbar^2}{2m_\alpha} \nabla_\alpha^2 + \frac{\hbar^2}{2M_T} \Big[\sum_{\substack{\beta=1 \\ \alpha \neq \beta}}^{N} \sum_{\alpha=1}^{N} \nabla_\alpha \cdot \nabla_\beta \tag{64}$$

$$+ 2 \sum_{\alpha=1}^{N} \sum_{i=1}^{n} \nabla_\alpha \cdot \nabla_i + \sum_{\substack{i=1 \\ i \neq j}}^{n} \sum_{j=1}^{n} \nabla_i \cdot \nabla_j \Big]$$

where

$$\mathcal{H}_{el} = - \frac{\hbar^2}{2m_e} \sum_{i=1}^{n} \nabla_i^2 + V^{el}(\underset{\sim}{r}_n, \underset{\sim}{R}_N) \tag{65}$$

where m_e, m_α, M_T, are the masses of the electron, atom α and combined system mass, respectively. Now since the ratios m_e/m_α and m_e/M_T are both small,

(2×10^{-6} - 5×10^{-4}) we can effect a separation of the electronic and nuclear coordinates treating the total wavefunction as a product of a nuclear and an electronic part. We have

$$\psi(\underset{\sim}{r}_n, \underset{\sim}{R}_N) = \sum_k \chi_k(\underset{\sim}{R}_N)\,\psi_k(\underset{\sim}{r}_n, \underset{\sim}{R}_N) \tag{66}$$

where $\psi_k(\underset{\sim}{r}_n, R_N)$ is an electronic wavefunction parametric in the nuclear coordinates as given in Equation (66) and $\chi_k(\underset{\sim}{R}_N)$ are nuclear motion wavefunctions which satisfy (neglecting terms of the order of m_e/m_α)

$$\left[-\sum_{\alpha=1}^{N} \frac{\hbar^2}{2m_\alpha}\nabla_\alpha^2 + \frac{\hbar^2}{2M_T}\sum_{\substack{\alpha=1\\ \alpha\neq\beta}}^{N}\sum_{\beta=1}^{N}\nabla_\alpha\cdot\nabla_\beta + V^{el}(\underset{\sim}{r}_n, \underset{\sim}{R}_N)\right]\chi_k = i\hbar\frac{\partial\chi_k}{\partial t} \tag{67}$$

The cross term in $\nabla_\alpha \cdot \nabla_\beta$ can be eliminated by a proper change of variables and Equation (67) then reduces to a 3N-3 dimensional Schrodinger equation.

For most systems, where the velocity of motion of the nuclei is slow relative to the electron velocity, this decoupling of electronic and nuclear motion is valid and is referred to as the adiabatic approximation. Equation (66) thus defines an electronic eigenstate $\psi_k(\underset{\sim}{r}_n, \underset{\sim}{R}_N)$, parametric in the nuclear coordinates, and a corresponding eigenvalue $E_k(\underset{\sim}{R}_N)$ which is taken to represent the potential energy curve or surface corresponding to state k.

In the usual ab initio method for calculating the electronic properties of a molecular system, one starts from a zero-order Hamiltonian that is exact except for relativistic and magnetic effects, and which involves the evaluation of electronic energies and other relevant quantities for wavefunctions that are properly antisymmetrized in the coordinates of all the electrons. For a system containing n electrons and M nuclei, the zero-order Hamiltonian depends parametrically on the nuclear positions and is of the form

$$\mathcal{H}_e = -\frac{1}{2}\sum_{i=1}^{n}\nabla_i^2 - \sum_{i=1}^{n}\sum_{j=1}^{M}\frac{z_j}{|\vec{r}_i - \vec{R}_j|} + \sum_{1\le i<j}^{M}\frac{z_i z_j}{|\vec{R}_i - \vec{R}_j|} + \sum_{1\le i<j}\frac{1}{|\vec{r}_i - \vec{r}_j|} \qquad (68)$$

where z_i and $\vec{R}_i$ are the charge and position of nucleus i, $\vec{r}_j$ is the position of electron j, and ∇_j^2 is the Laplacian operator for electron j. All quantities are in atomic units, i.e. lengths in bohrs, energies in hartrees (1 hartree = 2 Rydbergs).

In addition to the electrostatic contribution, $\mathcal{H}_e$, the complete Hamiltonian should contain additional terms which correct for magnetic interactions and relativisitic effects. These correction terms may be of importance in several applications. These include:

(1) calculation of the probability of making a transition from one quantum state to another in high-momentum collisions such as those that can occur in hot atom or heavy atom chemical dynamics experiments;

(2) determination of the interaction energy in heavy nuclei systems such as Cs_2 and UO^+, which exhibit open-shell structure on both nuclei at infinite internuclear separations;

(3) calculation of the intermolecular forces between free radicals, electronically excited states of molecules with open-shell structure, and long molecular conformations of possible biological interest.

3.1 BREIT-PAULI HAMILTONIAN

The relativistic correction terms to the usual electrostatic Hamiltonian have been derived through order α^2, where α is the fine structure constant, and are often referred to as the Breit-Pauli (Reference 42) Hamiltonian terms. This Hamiltonian has been derived by Bethe and Salpeter (Reference 43) for a two-electron system and has been generalized to the many-electron system by Hirschfelder, et al (Reference 44) and Itoh (Reference 45). In the absence of external electric or magnetic fields we can represent these correction terms as follows. Let $\vec{s}_j$ and $\vec{p}_j = \frac{1}{i}\Delta_j$ denote the operators for the spin and linear

moment of electron j, respectively. Then the generalized Breit-Pauli Hamiltonian, correct to terms of $O(\alpha^2/M)$, can be written as:

$$\mathcal{H}_{BP} = \mathcal{H}_e + \mathcal{H}_{LL} + \mathcal{H}_{SS} + \mathcal{H}_{LS} + \mathcal{H}_p + \mathcal{H}_D \tag{69}$$

where $\mathcal{H}_e$ is given by Equation (68) and the correction terms can be expressed as follows:

$$\mathcal{H}_{LL} = -\frac{1}{2} \sum_{1 \le k \le j} \frac{1}{r_{jk}^3} \left[r_{jk}^2 \, \vec{p}_j \cdot \vec{p}_k + \vec{r}_{jk} \cdot (\vec{r}_{jk} \cdot \vec{p}_j) \, p_k \right] \tag{70}$$

$$\mathcal{H}_{SS} = \sum_{1 \le k < j} \left\{ -\left(\frac{8\pi}{3}\right) \vec{s}_j \cdot \vec{s}_k \, \delta(\vec{r}_{jk}) + \frac{1}{r_{jk}^5} \left[r_{jk}^2 \, (\vec{s}_j \cdot \vec{s}_k) - 3 (\vec{s}_j \cdot \vec{r}_{jk})(\vec{s}_k \cdot \vec{r}_{jk}) \right] \right. \tag{71}$$

$$\mathcal{H}_{LS} = \frac{1}{2} \sum_{\alpha} \sum_{j} \left(\frac{Z_\alpha}{r_{j\alpha}^3}\right) (\vec{r}_{j\alpha} \cdot \vec{p}_j) \cdot \vec{s}_j - \frac{1}{2} \sum_{1 \le k \le j} \frac{1}{r_{jk}^3} \left[(\vec{r}_{jk} \times \vec{p}_j) \cdot \vec{s}_j - 2 (\vec{r}_{jk} \times \vec{p}_k) \cdot \vec{s}_j \right] \tag{72}$$

$$\mathcal{H}_p = -\frac{1}{8} \sum_j p_j^4 \tag{73}$$

$$\mathcal{H}_D = \frac{\pi}{2} \left[\sum_{\alpha} \sum_{j} Z_\alpha \, \delta(\vec{r}_{j\alpha}) - 2 \sum_{1 \le k < j} \delta(\vec{r}_{jk}) \right] \tag{74}$$

The first correction term, $\mathcal{H}_{LL}$, represents the magnetic orbit-orbit coupling terms of the electrons arising from the interaction of the magnetic fields created by their motion. The second term, $\mathcal{H}_{SS}$, gives the spin-spin magnetic coupling terms which are often quite appreciable. For $r_{jk} = 0$, only the delta-function contribution survives which represents the Fermi-contact spin interaction. The third term, $\mathcal{H}_{LS}$, is usually the largest in magnitude and represents the spin-orbit interaction between the spin and magnetic moment of each electron and the spin-other orbit interaction, which represents the coupling of the spin of one electron with the magnetic moment of a different electron. The term, $\mathcal{H}_{p}$, corrects for variation of the electron mass with velocity and the term, $\mathcal{H}_{D}$, represents electron spin terms identified by Dirac which appear to have no classical analogue.

Aside from the spin-orbit term, $\mathcal{H}_{LS}$, usually only the last term, $\mathcal{H}_{D}$, (often called the Darwin correction term) and $\mathcal{H}_{p}$, the mass-velocity term, are retained in the Hamiltonian, yielding the so-called Pauli approximation (Reference 43).

The eigenfunctions of the Hamiltonian represented by Equation (69) are four-component Dirac spinors which may be expressed as:

$$r\psi_{nkm} = \begin{pmatrix} P_{nk}(r)\ \chi_{km}(\theta,\phi) \\ iQ_{nk}(r)\ \chi_{-km}(\theta,\phi) \end{pmatrix} \tag{75}$$

where $\chi_{km}(\theta, \phi)$ are products of spherical harmonics and Pauli spinors and $P_{nk}(r)$, $Q_{nk}(r)$ represent, respectively, the large and small components of the radial wave equation. The exact solution of the Breit-Pauli Hamiltonian has only been given for one- and two-electron atomic systems (Reference 43) owing to the complexity of the operators for the general n-electron case. For a molecular system, Kolos and Wolniewicz (Reference 46) have calculated the relativistic corrections to H_2 using Equation (69) to $\mathcal{O}(\alpha^2)$. No heavier molecular systems have been treated using the full Breit-Pauli Hamiltonian.

3.2 APPROXIMATE TREATMENTS

Although the Breit-Pauli Hamiltonian given in Equation (69) can formally be employed in a molecular system, both the multiplicity of terms and the difficulty of evaluation of the resultant molecular integrals has precluded its general use to date. For atomic systems, various approximate methods of solution, within a Hartree-Fock or multiconfiguration Hartree-Fock framework, have been proposed for atoms (References 47-51). In most of these methods, a restricted Hamiltonian which includes only the one-electron Dirac terms is usually employed. The contributions of the Breit operators for spin-magnetic interactions and velocity retardation are then calculated as first-order perturbations using the zeroth-order Dirac relativistic wavefunctions.

An even more approximate method for incorporating the major relativistic effects has been proposed by Cowan and Griffin (Reference 52). In this method, the mass-velocity ($\mathcal{H}_p$) and Darwin ($\mathcal{H}_D$) terms, written in terms of the Pauli equation for one-electron atoms, are simply added to the usual non-relativistic Hamiltonian operator. In addition, the spin-orbit terms, $\mathcal{H}_{LS}$, are omitted, thereby reducing the system of equations to a single form representing the description of the major component wavefunction, $P_{nk}(r)$, evaluated at the center-of-gravity of the spin-orbit states. The rationale for this approximation lies in the observation that detailed atomic calculations using the complete DHF method have indicated that, even for an atom as heavy as uranium, less than 1 percent of the total charge is described by the small component radial wavefunctions.

The resulting equations have the form:

$$\left[-\frac{d^2}{dr^2} + \frac{\ell_i(\ell_i+1)}{r^2} + V^i(r) + H_m^i(r) + H_D^i(r) \right] G^i_{n\ell}(r) = \epsilon^i_{n\ell} G^i_{n\ell}(r) \qquad (76)$$

where the mass-velocity and Darwin terms take the form

$$H^i_m(r) = -\frac{\alpha^2}{4}\left[\epsilon^i - V^i(r)\right]^2 \tag{77}$$

$$H^i_D(r) = -\delta_{\ell_i,0}\ \frac{\alpha^2}{4}\left[1 + \frac{\alpha^2}{4}(\epsilon^i - V^i(r)\right]^{-1}\left[\frac{dV^i(r)}{dr}\left(\frac{d}{dr} - \frac{1}{r}\right)\right] \tag{78}$$

and $\alpha \tilde{=} 1/137.036$ is the fine structure constant. The spin-orbit term is omitted in Equation (76) and thus these equations represent center of gravity radial functions averaged over the two possible total angular momentum quantum numbers. Equation (76) represents (apart from the neglect of spin-orbit effects) the relativistic corrections to first order in α^2. A more accurate analysis of heavy atom energy levels and spectra is available through the use of the radial functions, $G^i_{n1}(r)$, found from Equation (76), and a first-order perturbation calculation. Cowan and Griffin (Reference 52) have illustrated the utility and accuracy of such an approach.

Recently, Wood and Boring (Reference 53) have adapted this approximate relativistic method to the local exchange problem and have implemented the solution of Equation (76) within the context of the multiple scattering Xα method (Reference 22). The central field Hamiltonian is modified to include mass-velocity and Darwin terms, given by Equations (77) and (78), in the sphere surrounding each atomic center. The intersphere region in the multiple scattering approach (constant potential region) is treated nonrelativistically since charge in this region is far from a nucleus and is screened by the charge concentrated around the atomic centers. The matching conditions for continuity of the wavefunction at the sphere boundaries permits any necessary charge transfer between the relativistic intra-atomic regions and the nonrelativistic interatomic constant potential regions. For an atom, the Wood-Boring treatment reduces to the Dirac-Slater local exchange method, but with the neglect of spin-orbit terms.

The implementation of Equation (76) into existing nonrelativistic multiple scattering molecular codes is facilitated by a change in the dependent variable, $G^{i}_{nl}(r)$, to eliminate the first derivative of the wavefunction, illustrated in Equation (78). The usual Numerov method of solution can then be applied to the central field problem; the only new requirement being the numerical tabulation of the first and second derivatives of the potential at each grid point in the integrations. These derivatives are computed only once for each complete SCF cycle and thus the total required computer time for a typical problem is not significantly increased as compared with a nonrelativistic calculation. A complete self-consistent program incorporating this method has been developed at UTRC. Our code has been tested by repeating calculations for the U and Pu atoms (Reference 52), where we find excellent agreement with the more exact, but cumbersome, Dirac-Slater calculations. Results for molecular calculations have recently been reported by Boring and Wood for UF_6 and UO_2^{++} (References 54 and 55). These calculations were carried out to illustrate the shifts in the valence levels for such systems resulting from relativistic effects. The total energy was not of principal concern.

We have recently reported (Reference 56) the first all-electron calculation of the potential energy curves for a molecule (Hg_2^{+}) built from atoms which exhibit significant relativistic effects. This study illustrated that reliable total energies are obtainable through a relativistic multiple scattering density functional treatment, provided care is taken to optimize potential match and overlap criteria for such systems. This study formed the basis of the computational scheme that we have employed here for the uranium/oxygen system.

3.3 EFFECTIVE CORE MODELS

It is well known from chemical experience that the outermost valence electrons contribute most to determining the chemical properties, especially spectroscopic properties, of molecules. The core electrons remain essentially unchanged from their atomic form except for internuclear separations of the order of the charge radii of the outer core region or less, wherein core polarization effects may become important. Since the computational time

required for ab initio calculations of electronic structure goes up at least quadratically with the number of electrons in the system, there have been many attempts to replace the more tightly bound core electrons with simple one-electron effective potentials (References 57-65). Concurrent with elimination of an explicit treatment of the core electrons, a transformation of the valence orbital basis is required to insure that the lowest valence orbital of each symmetry has a nodeless radial form, since it is well known that the lowest energy eigenfunction for a local potential must be nodeless (Reference 66).

Typical of the several effective core models that have been reported is that due to Kahn, et al (Reference 64) whereby an effective core potential is described in terms of angularly dependent projection operators as

$$U^{core} = U_L^{core}(r) + \sum_{\ell} \sum_{m} |\ell m\rangle \left[U_\ell^{core}(r) - U_L^{core}(r)\right] \langle \ell m| \qquad (79)$$

where L is taken at least as large as the highest angular momentum orbital occupied in the core. The term $U_L^{core}(r)$ represents the effective Coulomb and exchange potential felt by the valence electrons. The second term essentially accounts for the repulsive potential between valence and core electrons for each symmetry ℓ. The only non-local character exhibited by a potential of the form of Equation (79) arises from the ℓ-dependence which can be cast in terms of one-electron integrals between the core and valence orbitals. Explicit two-electron terms connecting core and valence orbitals are thus avoided which greatly simplifies the calculation of matrix elements of the effective Hamiltonian. The potential given by Equation (79) can be compared with the generalized Phillips-Kleinman pseudo-potential (Reference 59).

$$U^{core} = \sum_{c} (2J_c - K_c) + V^{CO} \qquad (80)$$

where J_c and K_c represent the core orbital Coulomb and exchange operators and V^{CO} is a complicated non-local operator which guarantees core-valence

orthogonality. Since the P-K core orbitals must simultaneously be eigenfunctions of both the core and valence Hartree-Fock Hamiltonians, V^{CO}, in general, contains complicated two-electron terms and limits the usefulness of Equation (80) over a full ab initio treatment.

The prescription of Kahn can be implemented by analytically fitting a nodeless pseudo-orbital, $\chi_{n\ell}$, to a linear combination of numerical or analytic Hartree-Fock orbitals determined from a full self-consistent treatment of the core electrons, using, for example, the multiconfiguration Hartree-Fock code of Froese-Fischer (Reference 67). The components, $U_\ell^{core}(r)$, of Equation (79) are then defined implicitly from the Schrodinger equation

$$\left[-\frac{\nabla^2}{2} - \frac{Z}{r} + U_\ell^{core}(r) + 2J_{val} - K_{val}\right] \chi_{n\ell} = \epsilon_{n\ell}\, \chi_{n\ell} \tag{81}$$

whereby

$$U_\ell^{core}(r) = \epsilon_{n\ell} + \frac{Z}{r} + \frac{1}{\chi_{n\ell}} \left[\frac{\nabla^2}{2} - 2J_{val} + K_{val}\right] \chi_{n\ell} \tag{82}$$

Equation (81) can be extended to relativistic systems in several ways. Kahn, et al (Reference 68) suggest an approximate treatment of adding only the mass-velocity and Darwin terms to the usual electrostatic Hamiltonian and to determine approximate HF orbitals in the manner prescribed by Cowan and Griffin (Reference 52). Equation (81) is then used to determine an effective $U_\ell^{core}(r)$ such that $\epsilon_{n\ell}$ are the eigenvalues of the CG approximate relativistic solution and $\chi_{n\ell}$ are curve-fitted to the CG-HF orbitals. In this treatment, the $\chi_{n\ell}$ represent approximate solutions to the major component wavefunction, $P_{n\ell}$, determined at the center-of-gravity of the spin-orbit states.

Lee, et all (Reference 65) adopt a somewhat more complicated treatment in which the spin-orbit operator is added to the usual electrostatic Hamiltonian,

in addition to the mass-velocity and Darwin terms retained in the Cowan-Griffin treatment. The large component eigenfunctions of a full Dirac-Hartree-Fock treatment of the atom, as given, for example, by Desclaux (Reference 69) are then curve-fitted in a manner similar to the Kahn treatment but include the additional index for the particular spin-orbit state, $\chi_{n\ell j}$. Use of these eigenfunctions in a molecular system fits more naturally into a (J-J) coupling scheme whereas the $\chi_{n\ell}$ determined using the Kahn method are more easily represented using Λ-s coupling.

Although these effective core models can often accurately describe an atomic eigenvalue sequence, including even high-lying electronically excited states (Reference 70), there are inherent difficulties in their application to molecular environments, where the maximum angular momentum component of the valence shell orbitals may often exceed the highest ℓ-value component retained in Equation (82). This is particularly true for valence orbitals which exhibit strong changes from atomic form through hybridization with higher angular momentum orbitals or through the addition of more compact polarizaiton terms. In either case, since the relativistic terms are now all buried in a fixed rather than a dynamic relativistic operator, only static core effects are imposed in determining the shape of the valence molecular orbitals. Relativistic effects between valence electrons and shielding effects of the core by the valence electrons are therefore neglected in these effective core treatments. In addition, the models obviously break down completely when the nuclei are brought together to dimensions such that core overlap and polarization effects become significant. Unfortunately, calculations to date seem to indicate that such effects begin to set in for internuclear separations of the order of equilibrium bond lengths.

SECTION 4

DISCUSSION OF RESULTS

An analysis of the electronic structure of UO and UO^+ using a relativistic formulation has previously been undertaken by UTRC (Reference 76). The possible low-lying molecular states are shown in Tables 1 and 2. Preliminary calculations were performed for several states of UO and UO^+ and for the ground state of UO_2, UO_2^+ and UO_2^{++}. A brief summary of the results of these molecular calculations follows.

UO

Electronic structure calculations were carried out for this system using a relativistic density functional formalism. Only a selected group of symmetries was studied. Our calculations indicate that the lowest symmetry of UO is derived from the (Λ,S) coupled ^5I state and has the following principal molecular orbital occupancy:

$$^5I \left[1\sigma^2\ 2\sigma^2\ 3\sigma^2\ 4\sigma^2\ 1\pi^4\ 2\pi^4\ \vdots\ 3\pi\ 1\delta\ 1\phi\ \vdots\ 5\sigma\right] \qquad (83)$$

The $\vdots\ 3\pi\ 1\delta\ 1\phi\ \vdots$ group derives from the $5f^3$ atomic configuration in the U atom and is quartet coupled. We have found that the ^5I state of UO is the ground state but that several other symmetries, including ^5K and ^3I, are low-lying. Our results indicate that only states of triplet or quintet multiplicity are bound for this system. An examination of the structure of these low-lying states of UO indicates a near total charge transfer to $U^{+2}O^{-2}$ for short (equilibrium) internuclear separations. Thus only the molecular states in the lower group shown in Table 1 are likely to be bound. This would yield 42 bound molecular states arising from $U\left[^5L\right] + O\left[^3P\right]$ and 39 repulsive states. Since (J-J) coupling is surely a better approximation for UO, these two manifolds of states will be optically connected and many pre-dissociation paths of the type:

$$UO^{*\ddagger} + h\nu \rightarrow UO^{**} \rightarrow U + O \qquad (84)$$

are possible. Here $UO^{*\ddagger}$ is a vibrationally excited low-multiplet state of UO and UO^{**} is a dissociating state. The predicted optical absorption should be strong since the transfer is from highly ionic states to neutral valence states of UO. Since UO has a large dissociation energy (7.87 eV), both one photon and two photon solar excitation processes are possible.

A vibrational analysis of the $\Omega = 5$ ground state of UO was carried out using a Hulbert-Hirshfelder (Reference 77) fit to our calculated potential curves. This fit yields an equilibrium internuclear distance of 1.89 Å and a fundamental vibrational constant (ω_e) of 859 cm^{-1}. The spin-orbit interaction was calculated using U^{+2} atomic splitting parameters. No explicit two-center effects are included. Our calculated spectroscopic data are compared in Table 3 with the theoretical work of Krauss and Stevens (Reference 78), the recent rotationally resolved experimental studies of Heaven and Nicolai (Reference 79), and estimates based on experimental data for similar systems. The agreement is well within the uncertainty of the calculations or experimental estimates. The theoretical studies predict a $^5I_5$ ground state for UO whereas the experimental data of Heaven and Nicolai suggest a $^5I_4$ ground state. The character of all of the low-lying multiplets of UO is similar however, and this apparent discrepency should not affect our conclusions about optical or LWIR absorptions.

An analysis of the LWIR emission from UO was carried out based on the ground ^5I electronic state. These calculations should also be representative of the LWIR emission from other low-lying electronic states since they exhibit similar ionicities. Our calculated f-numbers, including fundamentals and overtones, were reported in DNA-TR-82-159. These data ($v' > v''$) were given for the lowest 30 vibrational levels. For UO, our calculated f-number for the 1-0 transition is 4.86×10^{-5} at $\lambda = 12.04$ μ.

UO^+

Detailed searches of several symmetries of UO^+ were carried out to determine the ground molecular state of this system. Our calculations indicate that the lowest symmetry of UO^+ is derived from the (Λ, S) coupled ^4I state and has the following principal molecular orbital occupancy:

$$^4I\ [1\sigma^2\ 2\sigma^2\ 3\sigma^2\ 4\sigma^2\ 1\pi^4\ 2\pi^4\ \vdots\ 3\pi\ 1\phi\ 1\delta\ \vdots] \qquad (85)$$

Again we found that the $\vdots\ 3\pi\ 1\phi\ 1\delta\ \vdots$ group is quartet coupled in the ground state but a second manifold of states for the UO^+ system, which exhibit doublet coupling of these electrons, lies about 2 eV above the ground state. An apparent gap in the density of states for UO^+ is found between these two groups.

Calculations for UO^+ proved to be much more complex than UO owing to the presence of at least two low-lying dissociation limits of $U^+ + O$. As indicated in Table 2, the ionic $U^{++}O^-$ structures will mix in all multiplicities with molecular ion states arising from $U^+[^4I] + O[^3P]$, $U^+[^6L] + O[^3P]$, and $U^+[^6K] + O[^3P]$.

A vibrational analysis of the $\Omega = 9/2$ ground state of UO^+ was carried out using a Hulbert-Hirschfelder (Reference 77) fit to our calculated potential curves. The spin-orbit splittings were derived from atomic parameters for the U^{+3} ion. This fit yields an equilibrium internuclear distance of 1.84 Å and a fundamental vibrational constant of 890 cm^{-1}. These data are compared in Table 3 with other calculated estimates, since there are no experimental data available. The agreement between our work and that of Krauss and Stevens (Reference 78) is less satisfactory than in the case of UO but still well within the uncertainty of the several calculations.

A perturbative treatment for calculating the density of states in uranium molecules is available through the use of ligand field theory. The basic concept relies on the assumption that the structure and density of the 5f electrons in uranium and its ions remain unchanged in a molecular environment. Our calculated spin-orbit splitting for the 5f electrons in $U^{+3} \rightarrow U^{+5}$ is given in Table 4 where a comparison with earlier studies by Wood and Boring (Reference 53) is given. The overall agreement is excellent. In Table 5, we present the calculated excitation energies of several configurations of U^{+3}. These data clearly indicate that the ^4I component of $5f^3$ is low-lying and that the lowest doublet manifold lies ~ 2.2 eV above the ground state. If this

splitting carries over to the UO^+ ion without much change, the following solar pumped process is possible:

$$UO^+[^4I] + h\nu \rightarrow UO^{+*}[^2H] \tag{86}$$

$$e + UO^{+*}[^2H] \rightarrow U\,[^5L] + O[^3P] \tag{87}$$

Dissociative-recombination is not energetically possible from the ground ^4I state of UO^+ but it is possible from the excited ^2H and higher states. The optical connections between the manifolds of UO^+ states will be studied in future work.

An analysis of the emission characteristics for the ground state of UO^+ indicates an oscillator strength for emission (f_{10}) of 5.17×10^{-5} at λ = 11.3 μ. A complete analysis of our calculated LWIR emission for UO^+ was given in DNA TR-82-159. Our calculated LWIR emission for UO^+ is typical of that for a highly ionic metal oxide. We predict strong emission from the fundamentals of UO^+ in the wavelength region 11.3 ~ 14 μ. Since this system exhibits weak anharmonicity, we find the overtones down in intensity by several orders of magnitude. However, the first excited state of UO^+ (^4H) lies at ~ 2800 cm^{-1} in our calculations with a predicted electronic oscillator strength of ~ 1×10^{-5} for the $^4I - {}^4H$ transition. The electronic and vibrational manifolds for UO^+ are highly overlapped above the second vibrational level of the ground $^5I_{9/2}$ state. Since the density of electronic states of UO^+ is very large above ~ 2.2 eV, we predict that strong solar pumping, followed by intense radiation in the region $0.6 \lesssim \lambda \lesssim 11.3$ μ should occur for this system. This conclusion is similar to that reached by Krauss and Stevens (Reference 78) based on their MCSCF analysis of the UO^+ system. Since the excited electronic states of UO^+ lying in the region of strong solar flux (.4 - .7 μ) exhibit shifted equilibrium internuclear separation from that of the ground ^4I state, we predict efficient conversion of solar photons to IR photons for this system.

UO_2^+

An analysis of UO_2^+ has been carried out in $D_{\infty h}$ symmetry. McGlynn and Smith (Reference 80) have proposed a $^2\Phi_u$ ground state for this ion based on simple molecular orbital arguments. Their set of one-electron orbital energies is based on a maximum overlap criterion that is empirical in character. More modern calculations of the actinide series atoms suggest that a $U^{+5}[O^{-2}]_2$ or $U^{+3}[O^{-1}]_2$ structure should be the most stable configuration. In terms of MO's, the lowest predicted electronic state ($D_{\infty h}$) would be:

$$1\sigma g^2\ 1\sigma u^2\ 2\sigma g^2\ 1\pi u^4\ 2\sigma u^2\ 3\sigma g^2\ 2\pi u^4\ 1\pi g^4\ 3\sigma u^2 \mid 1\phi u : {}^2\Phi_u \qquad (88)$$

An extensive series of calculations of the possible low-lying symmetries of UO_2^+ now definitely establish this to be the ground state, but also predict a very low-lying $^2\Delta_u$ state.

A series of calculations of the low-lying electronic states of U^{+3}, U^{+4} and U^{+5} was first undertaken to determine the approximate location of the electronic states of the central ion which corresponded to f → d transitions. These results are given in Table 6 which indicate that f → d promotion in these ions lies at 327, 167 and 108 nm, respectively, for U^{+3}, U^{+4} and U^{+5}. This strong absorption (dipole-allowed), corresponding to central ion promotion, is predicted to occur only for wavelengths shorter than ~ 300 nm for UO_2^+. A spin orbit analysis of these calculated levels yields the splittings shown in Figure 1. The $^2\Phi_{5/2u}$ state is the predicted ground state multiplet.

In order to establish that f → d transitions in UO_2^+ lie at these short wavelengths, a series of molecular calculations of the low-lying electron states was undertaken. The promotion of an electron out of the $1\phi_u$ MO of UO_2^+, which is nearly purely U in composition, gives rise to the one-electron spectra shown in Table 7. The u → u intra-f-shell transitions are dipole-forbidden and correspond to the several weak absorption bands observed in solutions of UO_2^+ (Reference 81). The lowest dipole-allowed f → d transitions on the central uranium atom corresponds to the $^2\Phi_u$ (^5f_u) → $^2\Delta_g$ ($6d_g$) excitation at $\lambda \sim 300$ nm. This transition lies beyond the region of efficient solar

pumping of UO_2^+. Hay (Reference 82) reports a similar transition in his effective potential studies of UO_2^+, but at a somewhat shorter wavelength (~ 250 nm).

A separate molecular spectra for UO_2^+ arises from charge transfer states formed by promotion of an electron from (mainly) ligand MO's to a central uranium atom MO. Preliminary calculations (Reference 83) indicated that several of these states lie in the 300-400 nm region, and would therefore be efficiently solar pumped. A careful re-analysis of the ground $^2\Phi_u$ state indicated a false convergence onto local minima in the orbital parameter space. This produced a ground state potential curve with an internuclear separation that was too large, yielding excitation energies that were correspondingly too small. Careful convergence studies and the employment of a new integration scheme now gives an equilibrium U-O bond length in UO_2^+ of 1.73 Å. This value, coupled with a fundamental ν_3 vibrational frequency of 880 cm^{-1}, is now in good agreement with Badger's rule (Reference 84) correlating bond lengths and force constants for actinide salts and oxo-ions:

$$R(U\text{-}O) \simeq 1.08\ k^{-1/3} + 1.17 \qquad (89)$$

Using these more reliable integration methods, the low-lying charge transfer states of UO_2^+ were re-examined; their term levels are given in Table 8. These charge transfer states, some of which would exhibit very strong absorption, begin at ~ 47,000 cm^{-1} $[^4\Pi_u]$, with the first strong dipole allowed transitions corresponding to the excitation $1\pi g^4\ 1\phi u \rightarrow 1\pi g^3\ 1\phi u^2$. These transitions lie at 53,000 → 57,000 cm^{-1}, which correspond to absorption wavelengths in the VUV, well outside of the region for efficient solar pumping. A composite potential energy curve for UO_2^+, including both central uranium atom excitation states and the low-lying ligand to central atom charge transfer states, is given in Figure 2. Our calculated assignments of the f → f, f → d and charge transfer excitations among the low-lying states are given in Table 9.

This oxo-ion exhibits two different characteristic equilibrium U-O separations. They correspond to U^{+5} (O^{-2}) configurations with a short bond

and to U^{+4} $(O^{-15})_2$ charge transfer states which exhibit a weakened U-O bond and correspondingly longer equilibrium bond length. The spin orbit analysis for UO_2^+ is presently being carried out but this analysis will not affect our conclusion that solar pumping of electronically excited states of UO_2^+ has a low efficiency.

An analysis of the LWIR emission from UO_2^+ has been carried out based on the ground $^2\Phi_{5/2u}$ electronic state. These calculations should also be representative of the LWIR emission from other low-lying electronic states since they all exhibit similar ionicities. The spectroscopic data for the $^2\Phi_{5/2u}$ state, derived from our calcuated ground state potential curve, are shown in Table 10. We find a small anharmonicity in the IR active asymmetric ν_3 vibration, similar to that found in the highly ionic UO^+ and UO molecules. Our calculated f-numbers, including fundamentals and overtones are given in Table 11 for the lowest 30 vibrational levels. We have also included the emission wavelengths for each transition. For UO_2^+, our calculated f-number for the 1-0 transition is 1.2×10^{-4} at $\lambda = 11.43$ μ. This can be compared with a calculated f-number of 5.2×10^{-5} at $\lambda = 11.3$ μ for UO^+. Relatively strong LWIR is then predicted for UO_2^+. In Table 12, we present the calculated integrated band absorption coefficients as a function of temperature. All overtone contributions have been included in these band absorption coefficients.

$\underline{UO_2}$

An extensive set of calculations for the ground state of UO_2 was carried out in $D_{\infty h}$ symmetry. The ground electronic state has the dominant molecular orbital configuration:

$$^1\Sigma_g^+: \; [1\sigma g^2 \; 1\sigma u^2 \; 2\sigma g^2 \; 1\pi u^4 \; 2\sigma u^2 \; 3\sigma g^2 \; 2\pi u^4 \; 1\pi g^4 \; 3\sigma u^2 \; 1\phi u^2] \quad (90)$$

We find an equilibrium internuclear separation of 1.81 Å, a value somewhat larger than that corresponding to the various uranyl oxo-ions. At present it is uncertain whether this represents a deficiency in the calculations or whether significant back-bonding of electron charge to the central uranium atom is occurring in the gas phase UO_2 species. This would result in a lengthing of the U-O bond and a corresponding decrease in the U-O bond strength.

The first excited electronic state of UO_2 corresponds to a $1\phi u \rightarrow 3\pi u$ electron promotion. This state lies at ~ 1.4 eV but we predict very weak solar pumping since the transition is not dipole allowed. The first strongly allowed transition corresponds to a $1\phi u \rightarrow 1\delta g$ electron promotion at ~ 3.4 eV. This transition lies at ~ 360 nm putting it out of the region of efficient solar pumping. The LWIR analysis for neutral UO_2 should be carried out, however, since the highly ionic nature of UO_2 may give rise to a strong absorption/emission character for the asymmetric stretch vibrational mode.

SECTION 5

RECOMMENDATIONS

The low-lying molecular states of UO^+ arising from ^4I ($5f^37s^2$), $^6L(5f^37s6d)$, and $^6K(5f^37s6d)$ of U^+ are given in Table 2. Additional low-lying states of UO^+ arise from the $^6M(5f^36d7p)$ state of U^+ and from the doubly ionized $^5L(5f^36d)$ and $^5I(5f^37s)$ and triply ionized $^4I(^5f^3)$ states of the uranium ion. Further calculations of the term manifold for this molecular ion and doubly excited states of U^+ and UO^+ are needed in order to analyze the role of dielectronic recombination in this system. In our preliminary studies, a separate (higher lying) chemistry was found for U^+ when the 5f electrons were doublet spin-coupled. Verification of this structure, using a relativistic framework for this ion, is an area for future research activities.

Follow-on studies will also include an analysis of the several possible kinetic pathways that have been suggested by our work to date. These include photoexcitation and photodissociation of UO as:

$$\begin{aligned} U^+O^- + h\nu &\rightarrow UO^* \\ UO^* + h\nu &\rightarrow U + O \end{aligned} \qquad (91)$$

where UO* represents the excited neutral valence states of UO. Other potentially important kinetic studies include dissociative-recombination routes from

$$e + [UO^+]^* \rightarrow U^* + O \qquad (92)$$

where $[UO^+]^*$ is an electronically excited state of UO^+ which exhibits doublet coupling for the 5f electrons and charge transfer processes such as

$$U^{++} + O \rightarrow U^+ + O^+ \qquad (93)$$

In addition, the dissociative-recombination routes

$$
\begin{aligned}
e + UO^{++} &\rightarrow U^{+} + O \\
e + UO_2^{++} &\rightarrow U + O_2^{+} \\
&\rightarrow U^{+} + O + O \\
&\rightarrow UO + O^{+} \\
&\rightarrow UO + O
\end{aligned}
\qquad (94)
$$

are uncertain until the energetics of the doubly ionized UO^{++} and UO_2^{++} species are better defined.

In addition to these proposed calculations of the structure and radiative properties of uranium/oxygen species, an analysis of the importance of dielectronic recombination processes should be carried out. Dielectronic recombination (DR) is the process by which electron capture from the continuum to a bound state is facilitated by excitation of a previously bound electron. The process can be represented as:

$$
\begin{aligned}
e + U^{+} &\rightarrow [U]^{**} \\
[U]^{**} &\rightarrow [U]^{*} + h\nu
\end{aligned}
\qquad (95)
$$

where $[U]^{**}$ is a doubly excited continuum state of the neutral system and $[U]^{*}$ is a singly-excited Rydberg or Rydberg-like structure. A corresponding process is possible for $e + UO^{+}$. The low-lying doubly excited state structure of uranium begins at about 4600 cm^{-1}, indicating that this process needs to be considered for $T_e \gtrsim 3000$ °K. The region where $e + UO^{+}$ is important is unknown at the present time.

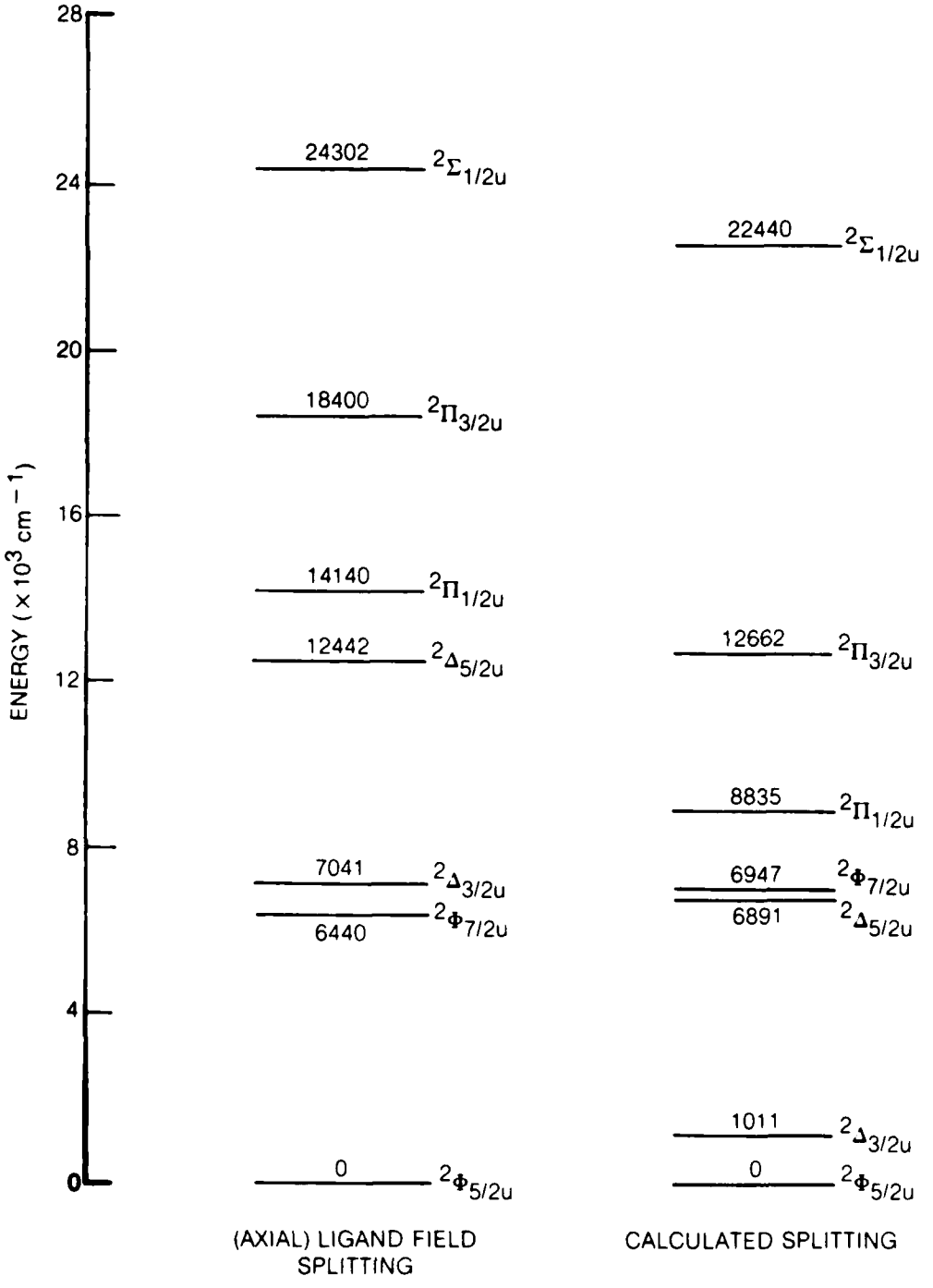

Figure 1. UO_2^+ energy levels — 5f splitting.

85-3-81-1

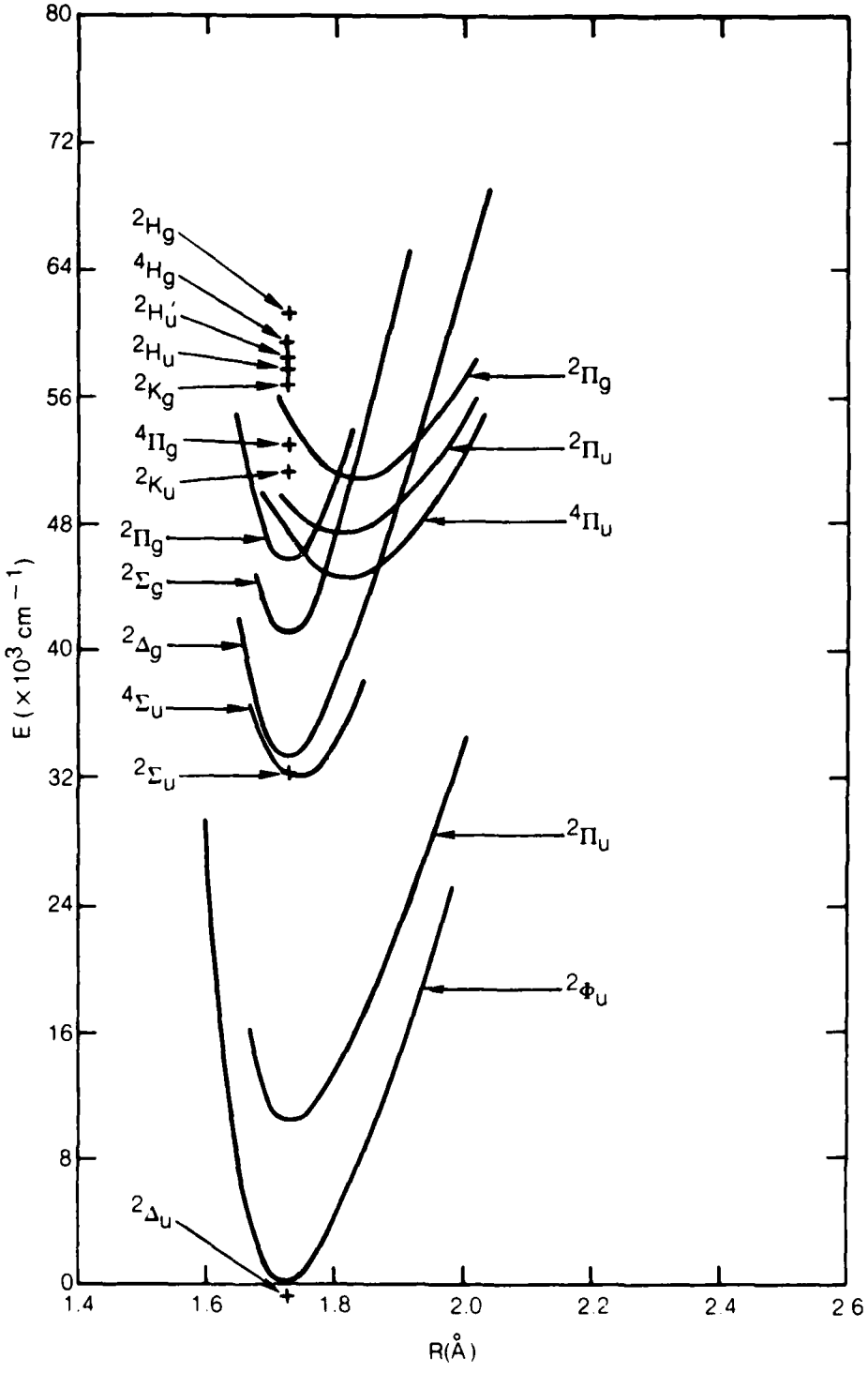

Figure 2. Potential energy curves for UO_2^+

85-3-81-2

Table 1. Molecular states of UO.

Separated Atom	Molecular States
U + O	
$^5L_u(5f^3 7s^2 6d) + {}^3P_g(2p^4)$ E_∞ = 0.000 eV (81 states)	$^3\Sigma^-(1)$, $^3\Sigma^+(2)$, $^5\Sigma^-(1)$, $^5\Sigma^+(2)$, $^7\Sigma^-(1)$, $^7\Sigma^+(2)$, $^3\Pi(3)$, $^5\Pi(3)$, $^7\Pi(3)$, $^3\Delta(3)$, $^5\Delta(3)$, $^7\Delta(3)$, $^3\Phi(3)$, $^5\Phi(3)$, $^7\Phi(3)$, $^3\Gamma(3)$, $^5\Gamma(3)$, $^7\Gamma(3)$, $^3H(3)$, $^5H(3)$, $^7H(3)$, $^3I(3)$, $^5I(3)$, $^7I(3)$, $^3K(3)$, $^5K(3)$, $^7K(3)$, $^3\Lambda(2)$, $^5\Lambda(2)$, $^7\Lambda(2)$, $^3M(1)$, $^5M(1)$, $^7M(1)$
$^5K_u(5f^3 7s^2 6d) + {}^3P_g(2p^4)$ E_∞ = 0.096 eV (72 states)	$^3\Sigma^-(2)$, $^3\Sigma^+(1)$, $^5\Sigma^-(2)$, $^5\Sigma^+(1)$, $^7\Sigma^-(2)$, $^7\Sigma^+(1)$, $^3\Pi(3)$, $^5\Pi(3)$, $^7\Pi(3)$, $^3\Delta(3)$, $^5\Delta(3)$, $^7\Delta(3)$, $^3\Phi(3)$, $^5\Phi(3)$, $^7\Phi(3)$, $^3\Gamma(3)$, $^5\Gamma(3)$, $^7\Gamma(3)$, $^3H(3)$, $^5H(3)$, $^7H(3)$, $^3I(3)$, $^5I(3)$, $^7I(3)$, $^3K(2)$, $^5K(2)$, $^7K(2)$, $^3\Lambda(1)$, $^5\Lambda(1)$, $^7\Lambda(1)$

Table 1. Molecular states of UO (Concluded)

Separated Atom	Molecular States
$U^+ + O^-$	
$^4I_u(5f^37s^2) + {}^2P_u(2p^5)$ (42 states)	$^3\Sigma^+(1)$, $^5\Sigma^+(1)$, $^3\Sigma^-(2)$, $^5\Sigma^-(2)$, $^3\Pi(3)$, $^5\Pi(3)$, $^3\Delta(3)$, $^5\Delta(3)$, $^3\Phi(3)$, $^5\Phi(3)$, $^3\Gamma(3)$, $^5\Gamma(3)$, $^3H(3)$, $^5H(3)$, $^3I(2)$, $^5I(2)$, $^3K(1)$, $^5K(1)$
$U^{++} + O^=$	
$^5L_u(5f^36d) + {}^1S_g(2p^6)$ (9 states)	$^5\Sigma^-(1)$, $^5\Pi(1)$, $^5\Delta(1)$, $^5\Phi(1)$, $^5\Gamma(1)$, $^5H(1)$, $^5I(1)$, $^5K(1)$, $^5\Lambda(1)$

Table 2. Molecular states of UO^+.

Separated Atom	Molecular States
$U^+ + O$	
$^4I_u(5f^3 7s^2) + {}^3P_g(2p^4)$ E_∞ = 6.11 eV (63 states)	$^2\Sigma^-(1)$, $^2\Sigma^+(2)$, $^4\Sigma^-(1)$, $^4\Sigma^+(2)$, $^6\Sigma^-(1)$, $^6\Sigma^+(2)$, $^2\Pi(3)$, $^4\Pi(3)$, $^6\Pi(3)$, $^2\Delta(3)$, $^4\Delta(3)$, $^6\Delta(3)$, $^2\Phi(3)$, $^4\Phi(3)$, $^6\Phi(3)$, $^2\Gamma(3)$, $^4\Gamma(3)$, $^6\Gamma(3)$, $^2H(3)$, $^4H(3)$, $^6H(3)$, $^2I(2)$, $^4I(2)$, $^6I(2)$, $^2K(1)$, $^4K(1)$, $^6K(1)$
$^6L_u(5f^3 7s6d) + {}^3P_g(2p^4)$ E_∞ = 6.146 eV (81 states)	$^4\Sigma^-(1)$, $^4\Sigma^+(2)$, $^6\Sigma^-(1)$, $^6\Sigma^+(2)$, $^8\Sigma^-(1)$, $^8\Sigma^+(2)$, $^4\Pi(3)$, $^6\Pi(3)$, $^8\Pi(3)$, $^4\Delta(3)$, $^6\Delta(3)$, $^8\Delta(3)$, $^4\Phi(3)$, $^6\Phi(3)$, $^8\Phi(3)$, $^4\Gamma(3)$, $^6\Gamma(3)$, $^8\Gamma(3)$ $^4H(3)$, $^6H(3)$, $^8H(3)$, $^4I(3)$, $^6I(3)$, $^8I(3)$ $^4K(3)$, $^6K(3)$, $^8K(3)$, $^4\Lambda(2)$, $^6\Lambda(2)$, $^8\Lambda(2)$, $^4M(1)$, $^6M(1)$, $^8M(1)$
$^6K_u(5f^3 7s6d) + {}^3P_g(2p^4)$ E_∞ = 6.223 eV (72 states)	$^4\Sigma^-(2)$, $^4\Sigma^+(1)$, $^6\Sigma^-(2)$, $^6\Sigma^+(1)$, $^8\Sigma^-(2)$, $^8\Sigma^+(1)$, $^4\Pi(3)$, $^6\Pi(3)$, $^8\Pi(3)$, $^4\Delta(3)$, $^6\Delta(3)$, $^8\Delta(3)$ $^4\Phi(3)$, $^6\Phi(3)$, $^8\Phi(3)$, $^4\Gamma(3)$, $^6\Gamma(3)$, $^8\Gamma(3)$, $^4H(3)$, $^6H(3)$, $^8H(3)$, $^4I(3)$, $^6I(3)$, $^8I(3)$, $^4K(2)$, $^6K(2)$, $^8K(2)$, $^4\Lambda(1)$, $^6\Lambda(1)$, $^8\Lambda(1)$

Table 2. Molecular states of UO^+ (Concluded)

Separated Atom	Molecular States
$U^{++} + O^-$	
$^5L_u(5f^36d) + {}^2P_u(2p^5)$ (54 states)	$^4\Sigma^+(1)$, $^4\Sigma^-(2)$, $^6\Sigma^+(1)$, $^6\Sigma^-(2)$, $^4\Pi(3)$, $^6\Pi(3)$, $^4\Delta(3)$, $^6\Delta(3)$, $^4\Phi(3)$, $^6\Phi(3)$, $^4\Gamma(3)$, $^6\Gamma(3)$, $^4H(3)$, $^6H(3)$, $^4I(3)$, $^6I(3)$, $^4K(3)$, $^6K(3)$, $^4\Lambda(2)$, $^6\Lambda(2)$, $^4M(1)$, $^6M(1)$
$U^{+++} + O^=$	
$^4I_u(5f^3) + {}^1S_g(2p^6)$ (8 states)	$^4\Sigma^-(1)$, $^4\Pi(1)$, $^4\Delta(1)$, $^4\Phi(1)$, $^4\Gamma(1)$, $^4H(1)$, $^4I(1)$, $^4K(1)$

Table 3. Calculated spectropic data for UO/UO$^+$

	UO $[^5I]$	UO^+ $[^4I]$
$\omega_e(cm^{-1})$:	820 (matrix)	949 (SCF)
	836 (scaled from ThO)	935 (MCSCF)
	863 (SCF)*	925 (MCSCF: Ω = 9/2)
	845 (MCSCF)**	980 (RDF-UTRC)
	859 (RDF-UTRC)	
$\omega_e X_e(cm^{-1})$:	2.7 (H-H potential)	2.7 (H-H potential)
	12.0 (^3I excited state)	
R_e(Å):	1.84 (matrix)	1.83 (SCF)
	1.838 (Heaven and Nicolai)**	
	1.88 (SCF)	1.84 (MCSCF)
	1.84 (MCSCF-Krauss)	1.84 (RDF-UTRC)
	1.89 (RDF-UTRC)	

*SCF and MCSCF results, see Reference 78.

** see Reference 79

Table 4. 5f spin-orbit parameters for U^{+n} ions

Configuration	ζ (cm^{-1}) LASL (Wood, Boring)*	RDF
U^{+5} ($5f$)	2442	2455
U^{+4} ($5f^2$)	2212	2220
U^{+3} ($5f^3$)	1977	1983

$$\zeta = \frac{2}{2\ell+1}\left(\varepsilon^{k} - \varepsilon^{k^*}\right);\ k^* = \ell \text{ for } j - 1/2$$

$$k = -(\ell + 1) \text{ for } j + 1/2$$

* Reference 53

Table 5. Term levels for U^{+3} ($5f^3$), cm^{-1}

Term	Energy
^2F	105180.
^2G	72366.
^2F	58586.
^2D	48896.
^2H	47659.
^2L	42749.
^4D	42566.
^2I	41939.
^2P	32066.
^2D	32060.
^2K	26419.
^4G	26097.
^2G	23665.
^2H	18222.
^4S	16782.
^4F	16653.
^4I	0.

$\overline{E_{avg}}$ = 33343 cm^{-1}.

Table 6. Excitation Energies of U^{+3}, U^{+4}, U^{+5}

	Configuration	E (cm^{-1})
U^{+3}	$5f^3_{5/2}$	0.
(ζ_{5f} = 1983 cm^{-1})	$5f^2_{5/2}\ 5f_{7/2}$	6938.
(ζ_{6d} = 2873 cm^{-1})	$5f_{5/2}\ 5f^2_{7/2}$	13898.
	$5f^3_{7/2}$	28890.
	$5f^2_{5/2}6d_{3/2}$	30592.
	$5f^2_{5/2}6d_{5/2}$	37774.
	$5f_{5/2}5f_{7/2}6d_{3/2}$	38166.
	$5f_{5/2}5f_{7/2}6d_{5/2}$	45342.
	$5f^2_{7/2}6d_{3/2}$	45754.
	$5f^2_{7/2}6d_{5/2}$	52938.
U^{+4}		
(ζ_{5f} = 2220 cm^{-1})	$5f^2_{5/2}$	0.
(ζ_{6d} = 3353 cm^{-1})	$5f_{5/2}5f_{7/2}$	7770.
	$5f^2_{7/2}$	15570.
	$5f_{5/2}6d_{3/2}$	60032.
	$5f_{5/2}6d_{5/2}$	68410.
	$5f_{7/2}6d_{3/2}$	68912.
	$5f_{7/2}6d_{5/2}$	77302.
U^{+5}		
(ζ_{5f} = 2455 cm^{-1})	$5f_{5/2}$	0.
(ζ_{6d} = 4268 cm^{-1})	$5f_{7/2}$	8592.
	$6d_{3/2}$	92921.
	$6d_{5/2}$	103590.

Table 7. Term levels for central atom (one-electron) excitation of UO_2^+

Molecular Orbital	Symmetry	Te (cm^{-1})
$1\phi u$	$^2\Phi_u$	0.
$1\delta u$	$^2\Delta_u$	-362.*
$3\pi u$	$^2\Pi_u$	10118.
$4\sigma g$	$^2\Sigma_u^+$	32250.
$1\delta g$	$^2\Delta_g$	33163.
$1\sigma g$	$^2\Sigma_g$	40976.
$2\pi g$	$^2\Pi_g$	45695.

* Although the center-of-gravity of the $1\delta u$ state lies lower than $1\phi u$, spin-orbit splitting causes the $^2\Phi_{5/2u}$ state to become the ground state, in agreement with previous studies of this system (Reference 81)

Table 8. Term levels for charge transfer states of UO_2^+

Molecular Orbital			Symmetry	Te (cm^{-1})
$2\pi_u^4$	$1\pi g^4$	$1\phi u$	$^2\Phi_u$	0.
$2\pi u^3$	$1\pi g^4$	$1\phi u^2$	$^4\Pi_u$	47341.
$2\pi u^3$	$1\pi g^4$	$1\phi u^2$	$^2\Pi_u$	49327.
$2\pi u^3$	$1\pi g^4$	$1\phi u^2$	^2K_u	51346.
$2\pi u^4$	$1\pi g^3$	$1\phi u^2$	$^4\Pi_g$	53080.
$2\pi u^4$	$1\pi g^3$	$1\phi u^2$	$^2\Pi_g$	55132.
$2\pi u^4$	$1\pi g^3$	$1\phi u^2$	^2K_g	56943.
$2\pi u^3$	$1\pi g^4$	$1\phi u\ 3\pi u$	^2H_u	58885.
$2\pi u^4$	$1\pi g^3$	$1\phi u\ 3\pi u$	^4H_g	59576.
$2\pi u^4$	$1\pi g^3$	$1\phi u\ 3\pi u$	^2H_g	61365.

Table 9. Calculated assignments of electronic transitions in UO_2^+

Transition	Wavelength	Strength
$^2\Phi_{5/2u} \rightarrow {}^2\Delta_{3/2u}$	> 5μ (calc)	Weak (u → u)
$^2\Phi_{5/2u} \rightarrow {}^2\Delta_{5/2u}$	1.5 - 1.6μ (calc)	Weak (u → u)
$^2\Phi_{5/2u} \rightarrow {}^2\Phi_{7/2u}$	1.45μ (calc)	Weak (u → u)
	~1.5μ (exp)	
$^2\Phi_{5/2u} \rightarrow {}^2\Pi_{3/2u}$	0.84μ (calc)	Weak (u → u)
	~0.9μ (exp)	
$^2\Phi_{5/2u} \rightarrow {}^2\Delta_{3/2g}$ (f → d)	0.30μ (calc)	Moderately Strong (u → g)
$^2\Phi_{5/2u} \rightarrow {}^2\Pi_{3/2g}$	0.18μ (calc)	Strong (u → g)
$(1\pi_g^4\ 1\phi_u \rightarrow 1\pi_g^3\ 1\phi_u^2)$		
$^2\Phi_{5/2} \rightarrow {}^4H_{5/2g}$	0.16μ (calc)	Very Strong (u → g)
$(1\pi_g^4\ 1\phi_u \rightarrow 1\pi_g^3\ 1\phi_u 3\pi_u)$		

Table 10. Calculated spectroscopic data for UO_2^+ - asymmetric mode

ω_3 (cm^{-1})	885.4
x_{33} (cm^{-1})	-2.7
r_e (Å)	1.73
D_e (cm^{-1})	62100. (exp)

Table 11. Calculated oscillator strengths ($f_{v'v''}$) for the vibrational transitions of UO_2^+

v'/v"		0	1	2	3	4	5	6	7	8	9
0		-	-	-	-	-	-	-	-	-	-
		-	-	-	-	-	-	-	-	-	-
1	*	1.17-04	-	-	-	-	-	-	-	-	-
	**	11.43	-	-	-	-	-	-	-	-	-
2		3.58-07	2.32-04	-	-	-	-	-	-	-	-
		5.73	11.50	-	-	-	-	-	-	-	-
3		2.20-09	1.07-06	3.47-04	-	-	-	-	-	-	-
		3.83	5.77	11.57	-	-	-	-	-	-	-
4		2.04-11	8.89-09	2.14-06	4.62-04	-	-	-	-	-	-
		2.88	3.86	5.81	11.65	-	-	-	-	-	-
5		3.11-13	1.03-10	2.19-08	3.56-06	5.75-04	-	-	-	-	-
		2.31	2.90	3.88	5.84	11.72	-	-	-	-	-
6		7.14-15	8.30-13	2.83-10	4.39-08	5.34-06	6.88-04	-	-	-	-
		1.93	2.33	2.92	3.91	5.88	11.79	-	-	-	-
7		6.43-15	1.66-14	4.32-12	6.67-10	7.73-08	7.48-06	8.00-04	-	-	-
		1.66	1.95	2.34	2.94	3.93	5.92	11.87	-	-	-
8		1.28-14	4.52-19	2.35-14	1.22-11	1.41-09	1.23-07	9.95-06	9.12-04	-	-
		1.46	1.67	1.96	2.36	2.96	3.96	5.95	11.95	-	-
9		1.42-17	7.34-15	8.49-17	5.37-13	2.53-11	2.48-09	1.85-07	1.28-05	1.02-03	-
		1.30	1.47	1.69	1.97	2.37	2.98	3.98	5.99	12.02	-

* oscillator strength

** wavelength, microns

Table 11. **Calculated oscillator strengths ($f_{v'v''}$) for the vibrational transitions of UO_2^+** (Continued)

v'/v"	0	1	2	3	4	5	6	7	8	9
10	8.37-15 1.18	1.70-15 1.31	3.39-14 1.48	3.14-15 1.70	3.81-13 1.98	5.23-11 2.39	4.00-09 3.00	2.64-07 4.01	1.59-05 6.03	1.13- 12.10
11	3.94-15 1.07	1.46-15 1.18	1.23-14 1.32	1.33-14 1.49	1.07-14 1.71	2.79-13 2.00	9.12-11 2.41	6.42-09 3.02	3.62-07 4.03	1.95- 6.07
12	4.41-16 0.99	1.45-15 1.08	8.84-15 1.19	7.26-18 1.33	3.91-14 1.50	1.56-14 1.72	1.83-12 2.01	1.50-10 2.42	9.83-09 3.04	4.82- 4.06
13	2.80-15 0.91	1.25-15 0.99	1.29-14 1.09	9.42-16 1.20	3.86-14 1.34	4.22-15 1.51	1.48-14 1.73	4.29-12 2.02	2.56-10 2.44	1.40- 3.06
14	6.77-16 0.85	8.44-15 0.92	2.93-16 1.00	1.79-14 1.09	3.07-15 1.21	2.38-15 1.35	9.18-16 1.52	5.22-14 1.74	4.36-12 2.04	4.01- 2.45
15	4.26-17 0.80	1.85-15 0.86	2.53-17 0.93	1.53-15 1.01	7.58-15 1.10	6.64-16 1.21	2.62-14 1.35	7.89-14 1.53	4.02-14 1.75	5.58- 2.05
16	3.20-16 0.75	1.99-15 0.80	7.17-17 0.86	1.19-14 0.93	4.37-16 1.01	1.71-14 1.11	6.99-15 1.22	4.87-15 1.36	1.26-13 1.54	2.99- 1.76
17	2.51-16 0.71	4.57-15 0.75	1.21-15 0.81	7.69-15 0.87	2.73-16 0.94	1.99-15 1.02	1.33-14 1.11	1.53-15 1.23	1.48-13 1.37	6.72- 1.55
18	8.06-17 0.67	6.56-16 0.71	5.59-15 0.76	1.05-16 0.81	6.06-15 0.87	1.23-14 0.94	8.02-17 1.03	4.03-14 1.12	3.11-15 1.24	5.73- 1.38
19	2.73-18 0.64	2.82-16 0.67	9.37-16 0.72	7.34-16 0.76	3.59-17 0.82	3.94-15 0.88	1.97-15 0.95	8.43-15 1.03	6.87-16 1.13	5.58- 1.25

Table 11. Calculated oscillator strengths ($f_{v'v''}$) for the vibrational transitions of UO_2^+ (Continued)

v'/v"	0	1	2	3	4	5	6	7	8	9
20	1.30-16	7.91-16	2.43-15	9.61-18	9.54-15	8.01-16	9.90-15	8.15-15	9.50-16	2.59
	0.61	0.64	0.68	0.72	0.77	0.82	0.88	0.96	1.04	1.14
21	1.61-16	4.69-16	5.15-15	6.16-16	3.08-15	6.16-17	4.72-16	3.65-15	6.86-15	3.65
	0.58	0.61	0.65	0.68	0.73	0.77	0.83	0.89	0.96	1.05
22	2.26-17	1.38-16	8.25-16	2.95-15	7.77-16	1.80-15	1.29-14	1.05-16	3.42-14	8.37
	0.56	0.58	0.62	0.65	0.69	0.73	0.78	0.83	0.90	0.97
23	2.30-17	2.26-18	4.02-16	5.33-16	1.23-15	6.85-16	2.08-15	7.30-15	8.09-15	3.88
	0.53	0.56	0.59	0.62	0.65	0.69	0.74	0.78	0.84	0.90
24	7.66-17	2.57-16	1.32-15	1.76-15	2.47-17	6.92-15	3.25-16	1.10-14	5.55-16	2.21
	0.51	0.54	0.56	0.59	0.62	0.66	0.70	0.74	0.79	0.85
25	4.04-17	4.71-16	8.06-16	4.41-15	1.73-16	1.48-15	3.98-16	1.75-16	3.98-16	1.69
	0.49	0.52	0.54	0.57	0.60	0.63	0.66	0.70	0.75	0.80
26	2.02-18	1.63-16	2.03-16	1.09-15	1.49-15	7.86-16	1.64-15	9.17-15	2.89-16	1.21
	0.48	0.50	0.52	0.54	0.57	0.60	0.63	0.67	0.71	0.75
27	6.29-18	1.41-17	1.68-18	1.92-16	5.64-16	9.04-16	7.94-16	2.63-15	6.55-15	7.60
	0.46	0.48	0.50	0.52	0.55	0.57	0.60	0.64	0.67	0.71
28	1.81-17	2.38-16	3.01-16	1.27-15	6.06-16	7.50-18	7.32-15	2.98-21	1.04-14	1.57
	0.45	0.46	0.48	0.50	0.53	0.55	0.58	0.61	0.64	0.68
29	1.63-17	2.47-16	6.88-16	1.00-15	2.88-15	1.06-16	2.40-15	6.28-16	6.58-16	5.72
	0.43	0.45	0.47	0.49	0.51	0.53	0.56	0.58	0.61	0.65

Table 11. Calculated oscillator strengths ($f_{v'v''}$) for the vibrational transitions of UO_2^+ (Continued)

v'/v"	10	11	12	13	14	15	16	17	18	19
10	-	-	-	-	-	-	-	-	-	-
	-	-	-	-	-	-	-	-	-	-
11	1.24-03	-	-	-	-	-	-	-	-	-
	12.18	-	-	-	-	-	-	-	-	-
12	2.33-05	1.35-03	-	-	-	-	-	-	-	-
	6.11	12.26	-	-	-	-	-	-	-	-
13	6.26-07	2.75-05	1.46-03	-	-	-	-	-	-	-
	4.09	6.15	12.35	-	-	-	-	-	-	-
14	1.92-08	7.95-07	3.21-05	1.56-03	-	-	-	-	-	-
	3.08	4.12	6.19	12.43	-	-	-	-	-	-
15	5.75-10	2.63-08	9.94-07	3.69-05	1.67-03	-	-	-	-	-
	2.47	3.10	4.14	6.24	12.51	-	-	-	-	-
16	1.08-11	8.49-10	3.51-08	1.23-06	4.21-05	1.78-03	-	-	-	-
	2.06	2.49	3.12	4.17	6.28	12.60	-	-	-	-
17	6.66-16	1.82-11	1.28-09	4.61-08	1.49-06	4.77-05	1.88-03	-	-	-
	1.78	2.08	2.50	3.14	4.20	6.32	12.68	-	-	-
18	6.74-14	2.83-13	3.39-11	1.80-09	5.97-08	1.79-06	5.36-05	1.98-03	-	-
	1.56	1.79	2.09	2.52	3.16	4.23	6.36	12.77	-	-
19	2.78-16	3.17-15	3.95-13	5.66-11	2.42-09	7.56-08	2.13-06	5.99-05	2.09-03	-
	1.39	1.57	1.80	2.11	2.54	3.18	4.26	6.41	12.86	-

Table 11. Calculated oscillator strengths ($f_{v'v''}$) for the vibrational transitions of UO_2^+ (Continued)

v'/v"	10	11	12	13	14	15	16	17	18	19
20	2.72-14 1.26	3.99-16 1.40	3.64-14 1.58	4.35-13 1.81	8.00-11 2.12	3.14-09 2.55	9.52-08 3.20	2.49-06 4.29	6.65-05 6.45	2.19-03 12.95
21	2.22-14 1.15	2.33-14 1.27	1.61-15 1.41	2.01-15 1.59	2.41-13 1.82	1.17-10 2.14	4.03-09 2.57	1.18-07 3.23	2.91-06 4.32	7.33-05 6.50
22	1.80-14 1.05	2.41-14 1.15	4.53-15 1.28	5.41-14 1.42	3.56-14 1.60	3.27-13 1.84	1.49-10 2.15	5.33-09 2.59	1.43-07 3.25	3.37-06 4.35
23	6.51-15 0.98	8.28-17 1.06	1.93-16 1.16	3.79-14 1.28	6.79-14 1.43	5.49-13 1.61	1.65-12 1.85	1.79-10 2.17	6.84-09 2.61	1.73-07 3.27
24	4.30-16 0.91	5.21-15 0.98	2.08-15 1.07	2.73-15 1.17	2.23-13 1.29	2.38-14 1.44	1.39-12 1.62	2.05-12 1.86	8.45-09 2.18	8.45-09 2.63
25	6.89-15 0.85	6.25-15 0.92	6.51-15 0.99	2.04-14 1.08	1.43-14 1.18	2.19-13 1.30	3.73-13 1.45	1.46-12 1.64	3.09-10 1.88	3.09-10 2.20
26	8.24-15 0.80	5.09-15 0.86	1.49-14 0.92	1.93-14 1.00	9.23-16 1.08	2.23-13 1.19	1.20-13 1.31	1.63-12 1.46	8.06-13 1.65	8.06-13 1.89
27	6.02-15 0.76	7.04-15 0.81	1.24-14 0.86	2.48-15 0.93	6.09-14 1.00	3.58-15 1.09	4.64-13 1.19	3.30-13 1.32	4.22-12 1.47	4.22-12 1.66
28	3.17-15 0.72	7.33-15 0.76	1.46-15 0.81	1.02-14 0.87	2.73-14 0.93	2.88-14 1.01	1.44-13 1.10	3.39-13 1.20	2.61-12 1.33	2.61-12 1.48
29	8.97-16 0.68	1.11-15 0.72	6.31-16 0.77	1.43-14 0.82	1.50-15 0.88	1.11-23 0.94	4.84-15 1.02	4.16-13 1.11	1.14-12 1.21	1.14-12 1.34

Table 11. Calculated oscillator strengths ($f_{v'v''}$) for the vibrational transitions of UO_2^+ (Concluded)

v'/v"	20	21	22	23	24	25	26	27	28	29
20	-	-	-	-	-	-	-	-	-	-
	-	-	-	-	-	-	-	-	-	-
21	2.29-03	-	-	-	-	-	-	-	-	-
	13.04	-	-	-	-	-	-	-	-	-
22	8.05-05	2.39-03	-	-	-	-	-	-	-	-
	6.54	13.14	-	-	-	-	-	-	-	-
23	3.87-06	8.81-05	2.49-03	-	-	-	-	-	-	-
	4.38	6.59	13.23	-	-	-	-	-	-	-
24	2.07-07	4.41-06	9.59-05	2.59-03	-	-	-	-	-	-
	3.30	4.41	6.64	13.33	-	-	-	-	-	-
25	1.04-08	2.45-07	5.02-06	1.04-04	2.69-03	-	-	-	-	-
	2.65	3.32	4.44	6.69	13.42	-	-	-	-	-
26	3.71-10	1.31-08	2.89-07	5.67-06	1.13-04	2.78-03	-	-	-	-
	2.21	2.67	3.34	4.47	6.74	13.52	-	-	-	-
27	2.17-12	4.74-10	1.61-08	3.42-07	6.39-06	1.21-04	2.88-03	-	-	-
	1.90	2.23	2.68	3.37	4.51	6.78	13.62	-	-	-
28	4.75-12	2.39-12	6.64-10	1.97-08	4.00-07	7.16-06	1.31-04	2.98-03	-	-
	1.67	1.92	2.25	2.70	3.39	4.54	6.83	13.72	-	-
29	4.22-12	3.09-12	4.60-12	8.43-10	2.42-08	4.64-07	7.98-06	1.40-04	3.07-03	-
	1.49	1.68	1.93	2.26	2.72	3.42	4.57	6.89	13.82	-

Table 12. Total integrated absorption coefficents for the UO_2^+ ground state

Temperature, °K (Wavelength, μ)	Absorption Coefficient, cm^{-2} atm^{-1} Fundamental (11.43)	First Overtone (5.73)	Second Overtone (3.83)	Third Overtone (2.88)	Total
100.	2773.12	8.51	0.05	0.00	2781.68
273.15	2772.97	8.68	0.05	0.00	2781.70
300.	2772.89	8.77	0.06	0.00	2781.71
500.	2771.71	10.01	0.07	0.00	2781.79
1000.	2766.50	15.31	0.14	0.00	2781.95
1500.	2760.16	21.61	0.27	0.00	2782.04
2000.	2753.40	28.23	0.45	0.01	2782.09
2500.	2746.39	35.01	0.69	0.02	2782.10
3000.	2739.19	41.90	0.99	0.03	2745.12
4000.	2724.32	55.95	1.78	0.07	2782.12
5000.	2708.17	70.16	2.81	0.15	2781.29

REFERENCES

1. Harang, O., "AlO Resonant Spectrum for Upper Atmosphere Temperature Determination," AFCRL-66-314, Environmental Research Paper, No. 192, 1966.
2. Churchill, D. R. and R. E. Meyerott, "Spectral Absorption in Heated Air," Journal of Quantitative Spectroscopy and Radiative Transfer, 5, p. 69, 1965.
3. The Airglow and the Aurorae, edited by E. B. Armstrong and A. Dalgarno. Pergamon Press, New York, 1955.
4. Armstrong, B. H., R. R. Johnston and P. S. Kelly,"The Atomic Line Contribution to the Radiation Absorption Coefficient of Air," Journal of Quantitative Spectroscopy and Radiative Transfer, 5, p. 55, 1965.
5. Johnston, R. R., B. H. Armstrong and O. R. Platas, "The Photoionization Contribution to the Radiation Absorption Coefficient of Air, "Journal of Quantitative Spectroscopy and Radiative Transfer, 5, p. 49, 1965.
6. Michels, H. H. and F. E. Harris, "Valence Configuration Interaction Calculations for Atomic Scattering, "International Journal of Quantum Chemistry, IIS, p. 21, 1968.
7. Harris, F. E. and H. H. Michels, "Open-Shell Valence Configuration - Interaction Studies of Diatomic and Polyatomic Molecules, "International Journal of Quantum Chemistry, IS, p. 329, 1967.
8. Michels, H. H., "Molecular Orbital Studies of the Ground and Low-Lying Excited States of the HeH^+ Molecular Ion," Journal of Chemical Physics, 44, p. 3834, 1966.
9. Michels, H. H., "Ab Initio Calculation of the $B^2\Sigma^+ - X^{2+}\Sigma$ Oscillator Strengths in AlO, Journal of Chemical Physics, 56, p. 665, 1971.
10. Michels, H. H., "Calculation of Electronic Wavefunctions," Final Report for AFOSR Contract F44620-74-C-0083, August 1975.
11. Michels, H. H., "Calculation of Potential Energy Curves for Metal Oxides and Halides, "Final Report for AFOSR, Contract F44620-73-C-0077, May 1977.
12. Michels, H. H., "Theoretical Determination of Metal Oxide f-Numbers," Final Report for AFWL, Contract F29601-71-C-0119, Report AFWL-TR-74-239, May 1975.

13. Schaefer, F. E. and F. E. Harris, "Ab Initio Calculations of 62 Low-Lying States of the O_2 Molecule," Journal of Chemical Physics, 48, p. 4946, 1968.

14. Michels, H. H. and F. E. Harris, "Predissociation Effects in the $A^2\Sigma^+$ State of the OH Radical," Chemical Physics Letters, 3, p. 441, 1969.

15. Harris, F. E., "Open-Shell Orthogonal Molecular Orbital Theory," Journal of Chemical Physics, 46, p. 2769, 1967.

16. Roothan, C. C. J. and P. S. Bagus, "Atomic Self-Consistent Field Calculations by the Expansion Method," Methods in Computational Physics. Edited by B. Alder, 2, p. 47, 1963.

17. Givens, W., "Eigenvalue-Eigenvector Techniques," Oak Ridge Report Number ORNL 1574 (Physics).

18. Shavitt, I., C. F. Bender, A. Pipano, and R. P. Hosteny, "The Iterative Calculation of Several of the Lowest or Highest Eigenvalues and Corresponding Eigenvectors of Very Large Symmetry Matrices," Journal of Computational Physics, 11, p. 90, 1973.

19. Harris, F. E. and H. H. Michels, "The Evaluation of Molecular Integrals for Slater-Type Orbitals," 13, p. 205, 1967.

20. Davidson, E. R., "Natural Expansion of Exact Wavefunctions, III. The Helium Atom Ground State," Journal of Chemical Physics, 39, p. 875, 1963.

21. Wahl, A. C., P. J. Bertoncini, G. Das and T. L. Gilbert, "Recent Progress Beyond the Hartree-Fock Method for Diatomic Molecules, The Method of Optimized Valence Configurations," International Journal of Quantum Chemistry, IS, p. 123, 1967.

22. Slater, J. C., Advances in Quantum Chemistry, 6, p. 1, 1972.

23. Löwdin, P. O., "Quantum Theory of Many-Particle Systems. I. Physical Intepretations by Means of Density Matrices, Natural Spin-Orbitals, and Convergence Problems in the Method of Configurational Interaction," Physical Review, 97, p. 1474, 1955.

24. Kohn, W. and L. Sham, "Self-Consistent Equations Including Exchange and Correlation Effects," Physical Review, 140A, p. 1133, 1965.

25. Slater, J. C., "A Simplification of the Hartree-Fock Method," Physical Review, 81, p. 385, 1951.

26. Schwarz, K.: "Optimization of the Statistical Exchange Parameters α for the Free Atoms H Through Nb, "Physical Review, B5, p. 2466, 1972.

27. Beebe, N. H. F., "On the Transition State in the X_α Method," Chemical Physics Letters, 19, p. 290, 1973.

28. Schwarz, K. and J. W. D. Connolly, "Approximate Numerical Hartree-Fock Method for Molecular Calculations," Journal of Chemical Physics, 55, p. 4710, 1971.

29. Connolly, J. W. D: unpublished results.

30. Slater, J. C., "Hellmann-Feynman and Virial Theorems in the X_α Method," Journal of Chemical Physics, 57, p. 2389, 1972.

31. Michels, H. H., R. H. Hobbs and J. C. Connolly, "Optimized SCF-X_α Procedures for Heterpolar Molecules," Journal of Chemical Physics (to be published).

32. Rosch, Notker and Keith H. Johnson, "On the Use of Overlapping Spheres in the SCF-X_α Scattered-Wave Method," Chemical Physics Letters, 23, p. 149, 1973.

33. Heitler, W., The Quantum Theory of Radiation. 3rd Edition, Oxford University Press, 1953.

34. Nicholls, R. W. and A. L. Stewart, Allowed Transitions. Atomic and Molecular Processes, D. R. Bates, Editor. Academic Press, 1962.

35. Penner, S. S., Quantitative Molecular Spectroscopy and Gas Emissivities, Addison-Wesley Publishing Company, Inc., 1959.

36. Dennison, D. M., "The Rotation of Molecules," Physical Review, 28, p. 318, 1926.

37. Kronig, R. and I. Rabi, "The Symmetrical Top in the Undulatory Mechanics," Physical Review, 29, p. 262, 1927.

38. Rademacher, H. and F. Reiche, "Die Quantelung des symmetrischen Kreisels nach Schrodingers Undulationsmechanik," Zeitschrift fur Physik, 41, p. 453, 1927.

39. Hönl, H. and F. London, "Intensities of Band Spectrum Lines," Zeitschrift fur Physik, 33, p. 803, 1925.

40. Herzberg, G., Spectra of Diatomic Molecules. 2nd Edition, Van Nostrand, 1950.

41. Fraser, P. A., "A Method of Determining the Electronic Transition Moment for Diatomic Molecules," Canadian Journal of Physics, 32, p. 515, 1954.

42. Breit, G., "The Effect of Retardation on the Interaction of Two Electrons. Physical Review, 34, p. 553, 1929; "The Fine Structure of He as a Test of the Spin Interactions of Two Electrons," 36, p. 383, 1930; "Dirac's Equation and the Spin-Spin Interactions of Two Electrons," 39, p. 616, 1932.

43. Bethe, H. A. and E. E. Salpeter, Quantum Mechanics of One- and Two-Electron Atoms. Academic Press, N. Y., 1957.

44. Hirschfelder, J. O., C. F. Curtiss and R. B. Bird, Molecular Theory of Gases and Liquids. John Wiley, N. Y., 1964.

45. Itoh, T., "Derivation of Nonrelativistic Hamiltonian for Electrons from Quantum Electrodynamics, "Reviews of Modern Physics, 37, p. 159, 1965.

46. Kolos, W. and L. Wolniewicz, "Accurate Adiabatic Treatment of the Ground State of the Hydrogen Molecule," Journal of Chemical Physics, 41, p. 3663, 1964; "Accurate Computation of Vibronic Energies and Some Expectation Values for H_2, D_2, and T_2," 41, p. 3674, 1964; "Potential-Energy Curve for the $B^1\Sigma u^+$ State of the Hydrogen Molecule," 45, p. 509, 1966.

47. Liberman, D., J. T. Waber, D. T. Cromer, "Self-Consistent Field Dirac-Slater Wave Functions for Atoms and Ions. I. Comparison with Previous Calculations," Physical Review, A137, p. 27, 1965.

48. Mann, J. B. and J. T. Waber, "SCF Relativistic Hartree-Fock Calculations on the Superheavy Elements 118-131," Journal of Chemical Physics, 53, p. 2397, 1970.

49. Grant, I. P.: "Relativistic Calculation of Atomic Structures," Advances in Physics, 19, p. 747, 1970.

50. Cowan, R. D.: "Atomic Self-Consistent-Field Calculations Using Statistical Approximations for Exchange and Correlation," Physical Review, 163, p. 54, 1967.

51. Desclaux, J. P., D. F. Mayers, and F. O'Brien, " Relativistic Atomic Wave Functions," Journal of Physics B, 4, p. 631, 1971.

52. Cowan, R. D. and D. C. Griffin, "Approximate Relativistic Corrections to Atomic Radial Wave Functions," Journal of the Optical Society of America, 66. p. 1010, 1976.

53. Wood, J. H. and A. M. Boring: "Improved Pauli Hamiltonian for Local-Potential Problems," Physical Review B, 18, p. 2701, 1978.

54. Boring, A. M. and J. H. Wood, "Relativistic Calculations of the Electronic Structure of UF_6," Journal of Chemical Physics, 71, p. 32, 1979.

55. Wood, J. H., A. M. Boring and S. B. Woodruff, "Relativistic Electronic Structure of UO_2^{++}, UO_2^{+} and UO_2," Journal of Chemical Physics, 74, p. 5225, 1981.

56. Michels, H. H., R. H. Hobbs and J. W. D. Connolly, "Electronic Structure and Photoabsorption of the Hg_2^{+} Dimer Ion," Chemical Physics Letters, 68, p. 549, 1979.

57. Weeks, J. D., A. Hazi and S. A. Rice: Advances in Chemical Physics, 16, p. 283, 1969.

58. Bardsley, J. N.: Case Studies in Atomic Physics, 4, p. 299, 1974.

59. Phillips, J. C. and L. Kleinman, "New Method for Calculating Wave Functions in Crystals and Molecules," Physical Review, 116, p. 287, 1959.

60. Hazi, A. U. and S. A. Rice, "Pseudopotential Theory of Atomic and Molecular Rydberg States," Journal of Chemical Physics, 45, p. 3004, 1966.

REFERENCES (Concluded)

61. Tully, J. C., "Many-Electron Pseudopotential Formalism for Atomic and Molecular Excited-State Calculations," Physical Review, 181, p. 7, 1969.

62. Melius, C. F., B. D. Olafson and W. A. Goddard III, "Fe and Ni Ab Initio Effective Potentials for Use in Molecular Calculations, "Chemical Physics Letters, 28, p. 457, 1974.

63. Szasz, L. and G. McGinn, "Atomic and Molecular Calculations With The Pseudopotential Method. II. Exact Pseudopotentials for Li, Na, K, Rb, Be^+, Mg^+, Ca^+, Al^{++}, Cu and Zn^+," Journal of Chemical Physics, 47, p. 3495, 1967; "Atomic and Molecular Calculations with the Pseudopotential Method III: The Theory of Li_2, Na_2, K_2, LiH, NaH and KH; Pseudopotential Theory of Atoms and Molecules. II. Hylleraas-Type Correlated Pair Functions for Atoms With Two Valence Electrons," 56, p. 1019, 1972.

64. Kahn, L. R., P. Baybutt and D.G. Truhlar, "Ab Initio Effective Core Potentials: Reduction of All-Electron Molecular Structure Calculations to Calculations involving Only Valence Electrons," Journal of Chemical Physics, 65, p. 3826, 1976.

65. Lee, Y. S., W. C. Ermler and K. S. Pitzer, "Ab Initio Effective Core Potentials Including Relativistic Effects. I. Formalism and Applications to the Xe and Au Atoms," Journal of Chemical Physics, 67, p. 5861, 1977.

66. Cowiant, R. and D. Hilbert, Methods of Mathematical Physics, Interscience, N.Y., 1961.

67. Froese-Fischer, C., Comp. Phys. Comm. 1, p. 151, 1969.

68. Kahn, L. R., P. J. Hay and R. D. Cowan, "Relativistic Effects in Ab Initio Effective Core Potentials for Molecular Calculations. Applications to the Uranium Atom," Journal of Chemical Physics, 68, p. 2386, 1978.

69. Desclaux, J. P.: Atomic Data and Nuclear Tables, 12, p. 311, 1973.

70. Krauss, M. O.: private communication.

71. Herman, F. and S. Skillman, Atomic Structure Calculations. Prentice-Hall, New Jersey, 1963.

72. Layzer, D., "On A Screening Theory of Atomic Spectra," Annals of Physics, 8, p. 271, 1959.

73. Kiess, C. C., C. J. Humphreys and D. D. Laung, J. Res. National Bureau of Standards, 37, p. 57, 1946.

74. Elliott, J. P., B. R. Judd and W. A. Runciman, "Energy Levels in Rare-Earth Ions," Proceeding of the Royal Society, A240, p. 509, 1957.

75. Judd, B. R., "Low-Lying Levels in Certain Actinide Atoms," Physical Review, 125, p. 613, 1962.

76. Michels, H. H. and R. H. Hobbs, "Theoretical Study of the Radiative and Kinetic Properties of Selected Metal Oxides and Air Molecules," Final Report for DNA Contract DNA001-82-C-0015, DNA-TR-82-159, July 1983.

77. Hulburt, H. M. and J. O Hirschfelder, "Potential Energy Functions for Diatomic Molecules," Journal of Chemical Physics, 9, p. 61, 1941.

78. Krauss, M. O. and W. S. Stevens, "The Electronic Structure and Spectra of UO^+, Chemical Physics Letters, to be published 1983.

79. Heaven, M. C., J. Nicolai, S. J. Riley and E. K. Parks, "Rotationally Resolved Electronic Spectra for Uranium Monoxide," to be published.

80. McGlynn, S. P. and J. K. Smith, "Electronic Structure, Spectra, and Magnetic Properties of Actinyl Ions. II. Neptunyl and the Ground States of Other Actinyls," Journal of Molecular Spectroscopy, 6, p.188, 1961.

81. Gritzner, G. and J. Selbin, "Studies of Dioxouranium (v) in Dimethylsulphoxide," Journal of Inorganic Nuclear Chemistry, 30, p. 1799, 1968.

82. Private communication.

83. Michels, H. H. and R. H. Hobbs, "Theoretical Study of the Radiative and Kinetic Properties of Selected Metal Oxides and Air Molecules," Progress Reports R83-926388-1 through R83-926388-5 and R84-926388-6 through R84-926388-7 for DNA Contract DNA001-83-C-0044, 1983 and 1984.

84. Badger, R. M., "The Relation Between the Internuclear Distances and the Force Constants of Molecules and Its Application to .olyatomic Molecules," 3, p. 710, 1935.

DISTRIBUTION LIST

DEPARTMENT OF DEFENSE

Assist to the Secy of Def, Atomic Energy
ATTN: Executive Assistant

Defense Intelligence Agency
ATTN: RTS-2B

Defense Nuclear Agency
ATTN: RAAE, P. Crowley
ATTN: RAAE, P. Lunn
ATTN: RAAE, K. Schwartz
4 cys ATTN: STTI-CA

Defense Technical Information Center
12 cys ATTN: DD

Field Command, DNA, Det 2
Lawrence Livermore National Lab
ATTN: FC-1

Field Command, Defense Nuclear Agency
ATTN: FCPR
ATTN: FCTT
ATTN: FCTT, W. Summa

Joint Strat Tgt Planning Staff
ATTN: JLKS

Under Secy of Def for Rsch & Engrg
ATTN: Defensive Systems
ATTN: Strat & Space Sys (OS)
ATTN: Strat & Theater Nuc For, F. Vajda

DEPARTMENT OF THE ARMY

Atmospheric Sciences Laboratory
3 cys ATTN: DELAS-EO, F. Niles

BMD Advanced Technology Center
ATTN: ATC-O, W. Davies
ATTN: BMDATC-D, M. Capps

BMD Systems Command
2 cys ATTN: BMDSC-HW

Dep Ch of Staff for Rsch Dev & Acq
ATTN: DAMA-CSS-N

Harry Diamond Laboratories
2 cys ATTN: DELHD-NW-P

US Army Ballistic Research Lab
ATTN: DRDAR-BLA-S, Tech Library
ATTN: DRDAR-BLB, J. Mester

US Army Combat Surv & Target Acq Lab
ATTN: DELCS-K, S. Kronenberg

US Army Foreign Science & Tech Ctr
ATTN: DRXST-SD

US Army Nuclear & Chemical Agency
ATTN: Library

US Army Research Office
ATTN: R. Mace

DEPARTMENT OF THE NAVY

Naval Intelligence Support Ctr
ATTN: Document Control

Naval Postgraduate School
ATTN: Code 1424 Library

Naval Research Laboratory
ATTN: Code 2000, J. Brown
ATTN: Code 2627, Tech Library
ATTN: Code 4128.2, J. Johnson
ATTN: Code 4139, D. McNutt
ATTN: Code 4700, W. Ali
ATTN: Code 4700, S. Ossakow
ATTN: Code 4720, J. Davis
ATTN: Code 4780, D. Strobel
ATTN: Code 6700, T. Coffey
ATTN: Code 6780, J. Fedder

Naval Surface Weapons Center
ATTN: Code F31
ATTN: Code X211, Tech Library

Space & Naval Warfare Systems Cmd
ATTN: PME 117-20

DEPARTMENT OF THE AIR FORCE

Air Force Geophysics Laboratory
ATTN: LSP, D. Smith
2 cys ATTN: LID, W. Swider
2 cys ATTN: LKO, R. Huffman
2 cys ATTN: LS, R. Murphy
2 cys ATTN: LSI, R. Sharma
2 cys ATTN: LSP, R. Nadile
2 cys ATTN: LYD, K. Champion
2 cys ATTN: OPR, D. Paulson
4 cys ATTN: CA, A. Stair

Air Force Office of Scientific Rsch
ATTN: AFOSR/NC
ATTN: AFOSRINP

Air Force Systems Command
ATTN: DLAE
ATTN: DLS
ATTN: DLTW
ATTN: DLXP
ATTN: SDR

Air Force Technical Applications Ctr
ATTN: TD
ATTN: Tech Library
ATTN: TF

Air Force Weapons Laboratory
ATTN: SUL

Air University Library
ATTN: AUL-LSE

Dep Ch of Staff, Rsch, Dev, & Acq
3 cys ATTN: AFRDS, Space Sys & C3 Dir

Rome Air Development Center
ATTN: OCD, J. Simons

DEPARTMENT OF THE AIR FORCE (Continued)

Space Division/AQ
ATTN: WE

Space Division
ATTN: YGD
ATTN: YN

Strategic Air Command
ATTN: SAC/SIJ
ATTN: INCR
ATTN: NRI/STINFO
ATTN: XPFR
ATTN: XPFS

DEPARTMENT OF ENERGY

Department of Energy
Office of Military Application, GTN
ATTN: OMA, DP-22

University of California
Lawrence Livermore National Laboratory
ATTN: L-10, A. Grossman
ATTN: L-10, H. Kruger
ATTN: L-262, D. Wuebbles
ATTN: L-325, G. Haugan
ATTN: L-48, E. Woodward
ATTN: L-71, J. Chang

Los Alamos National Laboratory
ATTN: D. Sappenfield
ATTN: G. Smith
ATTN: Librarian
ATTN: M. Pongratz
ATTN: M. Sanford
ATTN: MS362 Library
ATTN: R. Jeffries
ATTN: T. Bieniewski
ATTN: T. Kunkle, ESS-5

Sandia National Laboratories
ATTN: T. Cook

Sandia National Laboratories
ATTN: L. Anderson
ATTN: M. Kramm
ATTN: Org 1250, W. Brown
ATTN: Tech Library 3141

OTHER GOVERNMENT AGENCIES

Central Intelligence Agency
ATTN: OSWR/NED

Dep of Commerce, National Bureau of Standards
ATTN: A. Phelps

Dep of Commerce, National Bureau of Standards
ATTN: Sec Ofc for J. Devoe
ATTN: Sec Ofc for M. Krauss
ATTN: Sec Ofc for R. Levine
ATTN: Sec Ofc for S. Abramowitz

NASA, Goddard Space Flight Center
ATTN: Code 6801, A. Tempkin
ATTN: Code 900, J. Siry
ATTN: Tech Library
3 cys ATTN: A. Aikin

OTHER GOVERNMENT AGENCIES (Continued)

Dep of Commerce, Natl Oceanic & Atmospheric Admin
3 cys ATTN: E. Ferguson
3 cys ATTN: F. Fehsenfeld

Institute for Telecommunication Sciences
ATTN: G. Falcon
ATTN: W. Utlaut

NASA, George C. Marshall Space Flight Center
ATTN: J. Watts
ATTN: N. Stone
ATTN: W. Roberts

NASA, Ames Research Center
ATTN: N-245-3, R. Whitten

NASA, GSFC/WFF
ATTN: J. Gray

NASA Headquarters
ATTN: Schardt, Code EE

DEPARTMENT OF DEFENSE CONTRACTORS

Aero-Chem Research Labs, Inc
ATTN: A. Fontijn

Aerodyne Research, Inc
ATTN: C. Kolb
ATTN: J. Wormhoudt
ATTN: M. Camac
ATTN: M. Zahnhitzer

Aerospace Corp
ATTN: H. Mayer
ATTN: I. Garfunkel
ATTN: J. Reinheimer
ATTN: J. Straus
ATTN: V. Josephson
ATTN: N. Cohen

AVCO Everett Research Lab, Inc
ATTN: A830
ATTN: C. von Rosenberg, Jr
ATTN: Tech Library

Battelle Memorial Institute
ATTN: R. Thatcher
ATTN: STOIAC

Berkeley Rsch Associates, Inc
ATTN: J. Workman
ATTN: S. Brecht

Boston College, Space Data Analysis Lab
ATTN: E. Hegblom
ATTN: W. Grieder

The Trustees of Boston College
2 cys ATTN: Chairman Dept of Chemistry
2 cys ATTN: Chairman Dept of Physics

University of California at Riverside
ATTN: J. Pitts, Jr

California Institute of Technology
ATTN: J. Ajello

DEPARTMENT OF DEFENSE CONTRACTORS (Continued)

Calspan Corp
ATTN: C. Treanor
ATTN: J. Grace
ATTN: M. Dunn
ATTN: W. Wurster

University of Colorado
ATTN: C. Lineberger, JILA
ATTN: G. Lawrence, LASP

Computer Sciences Corp
ATTN: F. Eisenbarth

Concord Sciences Corp
ATTN: E. Sutton

Cornell University
ATTN: M. Kelly

University of Denver
ATTN: Sec Officer for D. Murcray

University of Denver
ATTN: B. van Zyl

Environmental Rsch Inst of Michigan
ATTN: IRIA Library

EOS Technologies, Inc
ATTN: B. Gabbard

General Electric Co
ATTN: P. Zavitsanos
ATTN: R. Edsall

Geo Centers, Inc
ATTN: E. Marram

HSS, Inc
ATTN: M. Shuler

Institute for Defense Analyses
ATTN: E. Bauer
ATTN: H. Wolfhard

IRT Corp
ATTN: H. Mitchell

JAYCOR
ATTN: H. Dickinson

Kaman Sciences Corp
ATTN: E. Conrad

Kaman Tempo
ATTN: B. Gambill
5 cys ATTN: DASIAC

Kaman Tempo
ATTN: DASIAC

Lockheed Missiles & Space Co, Inc
ATTN: B. McCormac
ATTN: J. Cladis
ATTN: J. Kumer
ATTN: J. Perez
ATTN: J. Reagan
ATTN: M. Walt
ATTN: R. Sears

DEPARTMENT OF DEFENSE CONTRACTORS (Continued)

Mission Research Corp
ATTN: D. Archer
ATTN: D. Sowle
ATTN: F. Guigliano
ATTN: M. Scheibe
ATTN: P. Fischer
ATTN: R. Hendrick
ATTN: R. Kilb
2 cys ATTN: Tech Library

Mission Research Corp
ATTN: C. Longmire
ATTN: R. Peterkin
ATTN: R. Stellingwerf

Nichols Research Corp, Inc
ATTN: R. Byrns

Pacific-Sierra Research Corp
ATTN: H. Brode, Chaiman SAGE

Photometrics, Inc
ATTN: I. Kofsky

Physical Dynamics, Inc
ATTN: A. Thompson

Physical Research, Inc
ATTN: T. Stephens

Physical Research, Inc
ATTN: J. Devore

Physical Science Lab
ATTN: W. Berning

Physical Sciences, Inc
ATTN: D. Greem
ATTN: G. Caledonia
ATTN: K. Wray
ATTN: R. Taylor
ATTN: T. Rawlings

University of the Commonwealth, Pittsburgh
ATTN: F. Kaufman
ATTN: M. Biondi
ATTN: W. Fite

Princeton University
ATTN: Librarian

R&D Associates
ATTN: F. Gilmore
ATTN: H. Ory
ATTN: R. Lindgren
ATTN: R. Turco

R&D Associates
ATTN: B. Yoon
ATTN: J. Rosengren

Rand Corp
ATTN: C. Crain
ATTN: P. Davis

Rand Corp
ATTN: B. Bennett

DEPARTMENT OF DEFENSE CONTRACTORS (Continued)

Science Applications Intl Corp
ATTN: D. Hamlin

Science Applications Intl Corp
ATTN: E. Hyman

Space Data Corp
ATTN: S. Fisher

SRI International
ATTN: C. Rino
ATTN: D. McDaniel
ATTN: J. Casper
ATTN: J. Vickrey
ATTN: President
ATTN: R. Leadabrand
ATTN: W. Chesnut

SRI International
ATTN: C. Hulburt

Stewart Radiance Laboratory
ATTN: R. Huppi

Technology International Corp
ATTN: W. Boquist

Teledyne Brown Engineering
ATTN: F. Leopard
ATTN: MS-12 Tech Library
ATTN: N. Passino

DEPARTMENT OF DEFENSE CONTRACTORS (Continued)

Toyon Research Corp
ATTN: J. Ise

United Technologies Research Ctr
2 cys ATTN: H. Michels
2 cys ATTN: R. Hobbs

Utah State University
ATTN: A. Steed
ATTN: C. Wyatt
ATTN: D. Baker
ATTN: K. Baker, Dir Atmos & Space Sci

VisiDyne, Inc
ATTN: J. Carpenter

Wayne State University
ATTN: R. Kummler

Wayne State University
ATTN: W. Kauppila

DIRECTORY OF OTHERS

Government Publications Library-M
ATTN: J. Winkler

Yale University
ATTN: Engineering Department